Lawrence Berkeley National Laboratory
LBL Publications

Title
Thermal performance and energy savings of white and sedum-tray garden roof: A case study in a Chongqing office building

Permalink
https://escholarship.org/uc/item/9k8075wd

Authors
Gao, Yafeng
Shi, Dachuan
Levinson, Ronnen
et al.

Publication Date
2017-12-01

DOI
10.1016/j.enbuild.2017.09.091

Peer reviewed

eScholarship.org Powered by the California Digital Library
University of California

This document is a pre-print of the following publication:

Gao, Y., Shi, D., Levinson, R., Guo, R., Lin, C., & Ge, J. (2017). Thermal performance and energy savings of white and sedum-tray garden roof: A case study in a Chongqing office building. *Energy and Buildings*, 156, 343–359. https://doi.org/10.1016/j.enbuild.2017.09.091

The pre-print may lack improvements made during the typesetting process. If you do not have access to the publication, you may request it from Ronnen Levinson at Lawrence Berkeley National Laboratory (RML27@cornell.edu).

HIGHLIGHTS

- Temperatures, heat flux and energy uses were measured in office building, Chongqing.
- Comparing white and sedum-tray garden roofs to black roof for one year.
- White roof reduced 1.6 times annual energy savings than sedum-tray garden roof.
- Natural aging of white and sedum-tray garden roofs has been discussed.

Thermal Performance and Energy Savings of White and Sedum-tray Garden Roof: A Case Study in a Chongqing Office Building

Yafeng Gao[a*], Dachuan Shi[b], Ronnen Levinson[c], Rui Guo[a], Changqing Lin[a], Jing Ge[c]

[a] National Centre for International Research of Low-carbon and Modular garden Buildings, Chongqing University, 400044, Chongqing, PR China

[b] Key Laboratory of the Three Gorges Reservoir Region's Eco-Environment, Ministry of Education, Chongqing University, 400044, Chongqing, PR China

[c] Lawrence Berkeley National Laboratory, 1CyclotronRoad, MS90R2000, Berkeley, CA94720,USA

[*] Corresponding author：

Email Adress: gaoyafeng79@126.com

Tel: +86 02365128079

Thermal Performance and Energy Savings of White and Sedum-tray Garden Roof: A Case Study in a Chongqing Office Building

ABSTRACT

This study presents the experimental measurement of the energy consumption of three top-floor air-conditioned rooms in a typical office building in Chongqing, which is a mountainous city in the hot-summer and cold-winter zone of China, to examine the energy performance of white and sedum-tray garden roofs. The energy consumption of the three rooms was measured from September 2014 to September 2015 by monitoring the energy performance (temperature distributions of the roofs, evaporation, heat fluxes, and energy consumption) and indoor air temperature. The rooms had the same construction and appliances, except that one roof top was black, one was white, and one had a sedum-tray garden roof. This study references the International Performance Measurement and Verification Protocol (IPMVP) to calculate and compare the energy savings of the three kinds of roofs. The results indicate that the energy savings ratios of the rooms with the sedum-tray garden roof and with the white roof were 25.0 % and 20.5 %, respectively, as compared with the black-roofed room, in the summer; by contrast, the energy savings ratios were −9.9 % and −2.7 %, respectively, in the winter. Furthermore, Annual conditioning energy savings of white roof (3.9 kWh/m^2) were 1.6 times the energy savings for the sedum-tray garden roof. It is evident that white roof is a preferable choice for office buildings in Chongqing. Additionally, The white roof had a reflectance of 0.58 after natural aging owing to the serious air pollution worsened its thermal performance, and the energy savings reduced by 0.033 kWh/m^2·d. Evaporation was also identified to have a significant effect on the energy savings of the sedum-tray garden roof.

Key Words

White roof; Sedum-tray garden roof; Office building; Thermal performance; Energy savings

Nomenclature

Q_a	air conditioning power demand intensity in one room (kW/m²)
Q_{load}	heat load of the tested room (kW/m²)
$Q_{envelope}$	heat gains from the roof, window, and other sources (kW/m²)
Q_{roof}	heat gain through the roof (kW/m²)
Q_e	heat gain within the room from other interior rooms (kW/m²)
Q_{window}	solar irradiance from the window (kW/m²)
Q_{other}	heat gain from other sources (e.g., plug load, infiltration, and occupants) (kW/m²)
Q_{wall}	heat gain from wall (kW/m²)
Q_{floor}	heat gain from floor (kW/m²)
ΔP	air-conditioning energy savings (kW)
ΔE	power savings of room (kWh)
P	air-conditioning energy consumption (kW)
E	power consumption of room (kWh)
$A_{adjustment}$	modification of energy savings (kWh)
ΔC	air-conditioning energy cost savings (RMB)
d_e	the price of electrical power (RMB/kWh)
Δp	CO_2 emission factor (tCO_2/MWh)
Q_m	measured air-conditioning energy consumption in one room (kW/m²)
$EF_{grid,2015}$	the mean marginal CO_2 emission factor in 2015 (tCO_2/MWh)

Greek Symbols

λ	thermal conductivity of interior wall (W·m /K)
δ	thickness of interior wall (m)
Δt	temperature difference between the opposite faces of interior walls (K)
τ	time (s)
A	the area of interior wall (m^2)

Subscript

a	air-conditioning
e	adjacent room
black	room with black roof
roof	room with white or sedum-tray garden roof
heating	heating season
cooling	cooling season

1. Introduction

As a result of economic growth and urbanization, buildings consume almost one-third of the total energy consumption and contribute to 40 % of the CO_2 emissions in China [1]. Especially, because the city's original surface has been replaced by black roofs and pavements (with an albedo of approximately 0.1 to 0.2), a shortage of greenery causes a decrease in canopy interception and transpiration in the city, leading to increased temperatures and CO_2 emissions. Worse still, in the summer, it results in urban heat islands (UHIs) and contributes to greater energy consumption, more heat-related deaths, increased peak-hour power demand, and other ecologically adverse impacts [2].

With the increase in the city's high-rise buildings and building density, the low-rise buildings are usually covered by other buildings, so the roofs are the major receivers of solar radiation in this case. Therefore, the insulation performance of the roof is an important factor affecting the thermal comfort and regional microclimate of low-rise buildings (e.g., podium buildings, old buildings, or factory buildings). In particular, the roof surface has a significant effect on the peak energy load and the total energy consumption of air-conditioned buildings, as well as the indoor thermal comfort in non-air-conditioned buildings [3]. The roofs of existing buildings usually consist of a waterproof membrane, insulation, and a structural layer [4], resulting in low reflectance and poorer insulation performance that makes the roofs inadequate to either reduce solar heat gains in summer or to decrease heat losses in winter [5]. The energy consumption due to the roof top accounts for 5 %–10 % of a building's total energy consumption (the more floors, the lower the percentage) and more than 40 % of the energy consumption of the top floor. These problems can be partially solved by retrofitting the rooftop construction. The technique of retrofitting common rooftop surfaces is often regarded as an effective strategy for rendering the buildings more sustainable [6] [7]. Specifically, innovative passive techniques such as cool (reflective) roofs and green (vegetative) roofs for improving the energy performance of buildings have demonstrated strategic environmental, economic, and social benefits [9].

These cool roofs can boost the albedo (solar reflectance) of the exterior surface of the buildings to reduce the solar heat gain, lower the surface temperature, and decrease the heat conduction through the roofs, thereby reducing the cooling load (albeit increasing the heating load) in a conditioned space, or lowering the air temperature in an unconditioned space [10]. Because of the added shade from the plants, the thermal resistance and thermal mass of the soil layer, and approximately 25 % of the solar radiation being consumed by the plants' evapotranspiration, only a small heat flux is transferred to the indoor space [11] [7] in the case of green roofs, which can improve the thermal performance of roofs and reduce the building's energy consumption in a cooling-dominated climate.

Normally, green roofs are classified as intensive, extensive, or semi-intensive [12]. An extensive roof is characterized by small plants, a thin soil layer (6–25 cm) and simple maintenance. An intensive roof, on the contrary, is heavier and thicker (15–70 cm) and requires more maintenance, while the semi-intensive roof falls in between these two [7]. Extensive roofs are often the preferred option for retrofitting old buildings [4]. However, extensive green roofs have displayed a few drawbacks such as heavy structural reinforcement requirements, drainage issues, high cost, and difficulties with design and construction [13]. In recent years, light sedum-tray garden roof has launched into the market to meet the need for a light-weight planting roof in urban areas [14]. In these systems, the plants initially grow in a freely combined container that is commonly made of PVC plastic. When the plants are more mature, they can be moved to the roof. This technology is not only easy to assemble and combine, but also keeps the roof structure intact to address the issues of storage and drainage, filtering, and preventing root overgrowth. Although it has been recognized in engineering practice, it has been rarely applied or studied.

In some countries, studies of white roofs have been conducted, in which the insulation performance and energy savings were analyzed based on the local climate and building form. White roofs can reflect 55–80 % of incident sunlight, making the roof surface stay cooler on clear summer days [13], which decreases the heat gain through the roof, lowers the indoor air temperature, and, thus, makes the indoor space more comfortable in unconditioned buildings; likewise, the white roof can also reduce the cooling load (although it increases the heating load) in a conditioned building. A. Synnefa et al. [16] investigated the application of white roofs to conditioned residential buildings in different climates, and discovered that the white roofs reduced the total cooling load and peak cooling load of conditioned rooms by 18 %–93 % and 11–27 %, respectively, and reduced the maximum temperature of the unconditioned buildings by 1.2–3.3 °C. Based on cool-roof studies performed in China and elsewhere, installing cool roofs is an effective way to reduce a building's energy consumption or improve its thermal comfort [40]. Moreover, white roofs can also reduce carbon emissions and neutralize global warming, as their highly reflective surfaces reflect an amount of radiation that would otherwise have been absorbed by the ground [16]. Cotana et al. estimated that approximately 16,000 tCO2-eq could be offset over 30 years with the installation of approximately 115,000 m^2 of white roofs at a Tunisian factory site [17]. Akbari et al. simulated the long-term effect of the increasing urban surface albedos using a spatially explicit global climate model of intermediate complexity; the results indicated that the global cooling ranged from 0.01 to 0.07 K, which corresponds to a carbon emission reduction of 25–150 billion tons of CO_2 [18].

However, a white roof faces the challenge of natural aging, which worsens its thermal insulation performance. Kelen et al. [19] researched the natural aging of roofs, 12 with standard paint and 8 with highly reflective paint, in São Paulo, Brazil. They found that the albedo of the roof tops sharply decreased, from 0.74 to 0.50, within their first 6 months due to climate and contamination and that a new cool roof could decrease the energy demand for cooling by 72 %, as compared to the aged cool roof. Elena et al. [20] found that the surface temperatures of white roofs after aging (with 0.50–0.55 reflectance) were higher than those of newly coated roofs (with 0.71–0.74 reflectance). The albedo of a white roof decreases due to local weather changes, wind erosion, microbial growth, and dust [21]. Chongqing, one of the first cities severely impacted by air pollution, including $PM_{2.5}$, O_3, haze, and smog, is in the Sichuan Basin and has complicated meteorology [22], so the natural aging there will be different than in other places. Compared with white roofs, sedum-tray garden roofs are less effective at reflecting incident light and have a lower global cooling potential. Coutts et al. [23] indicated that the reflectivity of a lighter-colored vegetated roof is 0.21. Similarly, Ekaterini and Dimitris [24] found that a vegetated roof had 27 % of its total solar radiation reflected, 60 % absorbed by the plants and the substrate medium, and a 13 % solar transmittance. Compared to white roofs, however, the albedo of sedum-tray garden roofs persists because of the life cycle of the plants, except for the reduction due to the contamination of the encapsulated polystyrene (EPS) base.

Sedum-tray garden roofs reduce a building's energy demand through the improvement of its thermal performance [25] [26]. Onmura [27] studied the roof of a three-story building in Osaka and found that implementing a sedum-tray garden roof could reduce the surface temperature and the heat flux of the roof by 30 °C and 50 %, respectively. The ability of green roofs to improve thermal performance was also reported by Ekaterini and Dimitris [28]. Sedum-tray garden roofs influence the roof surface and nearby air in two major ways [29]: they reduce the heat transfer into the top-floor rooms because of the insulating effect of their soil layer and vegetation, and the evaporation from the plants absorbs the sensible heat and transforms it into a latent heat of vaporization. A study in a hotel near Athens Beach in Greece measured that the roof surface and indoor temperatures of an unconditioned space were reduced by 14 °C and 3 °C, respectively, owing to the implementation of a green roof, and a simulation of the whole building indicated that the green roof could reduce the cooling load by 45–61 %, heating load by 45 %, and annual power demand by 37–48 %. According to their findings, strengthening the ventilation of the unconditioned space at night could further enhance the cooling effect of the sedum-tray garden roofs [30].

However, the energy savings of sedum-tray garden roofs are totally different in different climates because of hydrological performance and other factors. For instance, during the winter, the green roof acts as an insulator and decreases the heat flow, although this benefit has been often-debated. Some studies have claimed that a green roof saved energy [31], some identified that a green roof had no influence on energy consumption during the winter [32], while still others viewed it as the cause of increased energy consumption [33]. Researchers in Japan found that the peak sensible heat fluxes (Q_H) were small for the white roof (153 W/m^2) during a summer day, but the Q_H of the green roof was twice as much as that of the white roof [34]. However, Scherba et al. [35] modeled the performance of green and white roofs and found that the daily Q_H was not that much greater for the green roofs. We think that the thermal performance and energy savings are strongly affected by the climate and hydrology and that a lack of local research and the premature introduction of products into the market causes the sedum-tray garden roofs to generally not be optimized to realize their benefits [36]; therefore, it is necessary to conduct local research of sedum-tray garden and white roofs in China, as well as to provide a comprehensive comparison between these two roof types[37].

Above all, white roofs and sedum-tray garden roofs can provide numerous economic and social benefits in addition to their more-obvious environmental advantages [38] [39] [40]. Hence, the Chinese government has started promoting the implementation of white and sedum-tray garden roofs on buildings. Notably, while the related products have started to thrive in China, many benefits have not yet been fully realized through engineering due to the lack of local research in following areas: 1) there have been some case studies that compared white roofs with black roofs [41] [42] [43] and green roofs with black roofs [44] [45], but there is no systematic comparative study on the energy savings of these two roof types in Chongqing, China; 2) there is a lack of study on the attenuation of albedo through the natural aging of the two roof types in significant air pollution; 3) there is no comparative study of the energy efficiency before and after the natural aging in China; and 4) for the new type of light-weight sedum-tray garden roof, there is a lack of study on its thermal performance and energy savings.

This case study analyzes the heat transfer mechanisms of white and sedum-tray garden roofs and the energy savings realized between September 2014 and September 2015 for three air-conditioned rooms (rooms A, B, and C) of an office building in Chongqing, China, which is a typical hot and humid climate in which offices use air conditioning between May and September, by monitoring energy performance (temperatures, heat fluxes, and energy consumption) and the external roof temperatures. We also reference the IPMVP for savings determination. Additionally, the impact of natural aging upon the energy efficiency of the two roof types is also considered.

2. Theoretical analysis

Although the tested rooms shared the same floor, their fenestration (orientation, window area, construction, and shadings), plug load (air-conditioning system, lighting, and occupancy), and other differences beyond their roof construction could influence their air conditioning energy consumption. In this study, we analyzed the heat balance model, and then referenced the IPMVP to synthetically evaluate the cumulative energy savings and peak-hour power demand reduction, along with the energy cost savings and emission reduction, and, finally, the comprehensive operational conditions and economic benefits attributable to the white roof and sedum-tray garden roof.

2.1. Heat balance model

A tested room can gain or lose heat through both its envelope (e.g., roof, window, walls, and floor) and interior walls with no internal sources, as the air-source heat pump removes cooling or heating loads to maintain thermal comfort. Denoting the rates of heat gain (power) from other interior rooms, the room's envelope and other sources as Q_e , $Q_{envelope}$ and Q_{other}, respectively, the rate Q_{load} at which the heat pump must remove heat to regulate the room's air temperature, Q_{load} (positive in cooling season, negative in heating season) is disaggregated into heat gain through envelope (e.g., wall, roof, window, and floor), other sources (e.g., plug load, infiltration, and occupants) and heat transfer through interior rooms:

$$Q_a = Q_{load} = Q_{envelope} + Q_{other} + Q_e$$

(1)

Q_{envelope} is disaggregated into heat gain through envelope (e.g., wall, roof, window, and floor), other sources (e.g., plug load, infiltration, and occupants) and heat transfer through interior rooms, such that [46]:

$$Q_{load} = Q_{envelope} + Q_{other} + Q_e = Q_{wall} + Q_{roof} + Q_{window} + Q_{floor} + Q_{other} + Q_e \quad (2)$$

Eqs. 2 is the heat balance model of tested rooms. The subscript of the rate represents the source of heat gain, Q_{roof} can be measured by roof heat flux. Q_{window} can be estimated by a U value (3.94 W/m²K) of a window and a g-value (0.50). Q_e is calculated by indoor air temperatures of adjacent rooms.

Because the three air-source heat pumps share the same coefficient of performance (COP), we define the rate of air-conditioning heat removal during the cooling season and heating season, respectively, as:

$$Q_{a,cooling} = COP_{cooling} \cdot P_{cooling} \quad (3)$$

$$Q_{a,heating} = COP_{heating} \cdot P_{heating} \quad (4)$$

Considering that the three tested rooms in the office building have the same envelope and construction, except for the different roof types (black, white, and sedum-tray garden roof), we define:

$$\Delta P \equiv P_{black} - P_{roof} \tag{5}$$

Together with Eqs. (3), (4), and (5), the air-conditioning power savings during the cooling and heating seasons (positive during the cooling season, negative during the heating season) is:

$$\Delta P = \frac{\Delta Q_a}{COP} = \frac{\Delta Q_{load}}{COP} \tag{6}$$

For distinguishing the air-conditioning power savings of the roof from those aspects, we define the air-conditioning power savings due to the white roof and sedum-tray garden roof during the cooling and heating seasons (positive during the cooling season, negative during the heating season) as:

$$\Delta P_{roof} = \frac{\Delta Q_{roof}}{COP} \tag{7}$$

We calculate the air-conditioning power savings from the measured power consumption denoted as Q_m for one room, in consideration of the heat transfer through interior walls. If we assume the envelope of all tested rooms is well insulated, such that $\Delta Q_{other} = 0$, then combining Eqs. 2, 6 and 7 yields the cooling and heating power savings (positive in healing season, negative in cooling season) is:

$$\Delta P_{roof} = \Delta P \pm \frac{\Delta Q_{window} + \Delta Q_{wall} + \Delta Q_{floor} + \Delta Q_e}{COP} \tag{8}$$

2.2. Energy savings

The IPMVP provides a procedure for comparing the energy consumption levels before and after the application of energy conservation measurements (ECMs). The comparison of before and after energy consumption or demand should be made on a consistent basis, using the following general equation [47]:

$$\Delta E = (E_{baseline} - E_{reporting}) \pm A_{adjustments} \tag{9}$$

where $A_{adjustments}$ is used to remove the air conditioning heat load transfer caused by the interior wall heat transfer from the simple comparison of cost or usage before and after the implementation of an energy conservation measure (ECM).

The IPMVP provides four options (A, B, C, and D) for determining energy savings. Option C is best applied where the ECMs involve activities for which the individual energy consumption is difficult to measure separately (e.g., operator training and wall or window upgrades), so this is the option chosen for use in this case study [48].

Option C in the IPMVP compares the energy consumption, adjusted for weather and other interfering factors, before and after the ECMs, but this case used parallel controlled measurements in rooms A, B (black roof as baseline), and C, which objectively negated the differential influence of the weather and other interference factors [49]. However, the power consumption must still be adjusted to account for the energy effects of the heat transfer through the interior walls of these three different rooms. Except for the differences in the time and space dimensions, the experimental objects (i.e., the cooling and heating temperatures and the air conditioning energy consumption) are the same as the IPMVP Option C. Therefore, when referencing the IPMVP Option C to calculate the energy savings, each month's energy consumption (for the white and sedum-tray garden roofs) required modification to account for the interior wall heat transfer, which was then taken from the corresponding baseline actual demand (black roof). Then, the equation (6) could be transformed to:

$$\Delta E = (E_{black} - E_{roof}) \pm A = \int \Delta P dt \pm A_{adjustment} \tag{10}$$

Such that, once the expressions of $A_{adjustment}$ for the cooling and heating seasons were derived, the Q_e could be analyzed.

The interior wall heat transfer process can be viewed as a one-dimensional heterogeneous partition unsteady heat conduction process [50]. In this study, the interior wall heat transfer is approximated as a steady-state heat transfer in five-minute increments, then summed by the hour, so that the daily interior wall heat transfer during the test period could be calculated. The energy consumption of the interior wall heat transfer is:

$$Q_e = \int_{day} \lambda A(\Delta T / \Delta x)dt = -300\sum_{i=1}^{288} \lambda A(\Delta t / \delta)\tau_i \quad (11)$$

In practice, the energy savings effects of the white and the sedum-tray garden roofs may be affected by the heat radiation intensities between the interior surfaces and interior walls of these three different rooms. Thus, the energy consumption in the different test rooms can be expressed in the following way when the heat transfer between the rooms is considered [46]:

$$Q_a = Q_m + Q_e \quad (12)$$

Hereto, under the condition of a well-insulated envelope, the daily, seasonal, and annual cumulative energy savings of the rooms are each evaluated using Eqs. (8), (9), and (11).

2.3. Other savings and emissions reductions

2.3.1 Energy cost savings

The air conditioning energy cost savings for a period (daily, seasonally, or annually) can be calculated as:

$$\Delta C = d_e \cdot \Delta E \quad (13)$$

where d_e is the prices of electricity, is cumulative energy savings of rooms. ΔE is the power savings of room and calculated by Eqs. 10 and 11.

2.3.2 Emissions reductions

The reduction of CO_2 emissions can be calculated as:

$$\Delta p = EF_{grid,2015} \cdot \Delta E \quad (14)$$

where $EF_{grid,2015}$ is the mean marginal emissions factor in 2015 and is derived by taking a weighted average of the values of $EF_{grid,OM,2015}$ and $EF_{grid,BM,2015}$ [51], which are obtained from the *2015 Baseline Emission Factors for Regional Power Grids in China;* Chongqing belongs to the Central China Grid [52].

2.3.3 Peak-hour power demand reduction

The peak electrical demand could be defined by the utilities. According to the *Chongqing Power Grid Peak and Valley Load Trial Measures for Electricity (2000)*, the State Grid Chongqing

Electric Power Company and the Chongqing Municipal Price Bureau classify 08:00–12:00 and19:00–23:00 local standard time (LST) as the peak demand hours for ordinary non-residential users [53]. Therefore, the value of the cooling energy saved during 08:00–12:00 LST could be used to measure the peak-hour demand reduction in the office building for one daytime period.

3. Experimental study

3.1. Study location

Chongqing, a mountain city located in southwest China, has a subtropical humid monsoon climate, with hot summers, cold winters, and high humidity throughout the year, owing to the shielding effect of the mountains around the Sichuan Basin and the influence of the Qinghai-Tibet Plateau [57]. Solar radiation is primarily distributed in the summer, and is up to 4 times greater than that in the winter, ranging from 121.2 W/m^2 in January to 558.8 W/m^2 in September. As shown in Figure 1, the mean annual temperature is 18.6 °C, and the maximum outdoor air temperature is up to 28.5 °C higher in the summer than in the winter, ranging from about 7.5 °C in December to 35.8 °C in June.

Figure 1 Mean outside air temperature and global solar irradiance through the year.

Figure 2 illustrates that Chongqing features a hot and humid climate (relative humidity greater than 70 % in all months), with a mean annual relative humidity of 78.9 %, and a maximum relative humidity of 85.9 % in December. Fog and haze frequently occur in Chongqing, because of low wind speed and high levels of air pollution, including $PM_{2.5}$ and O_3; the $PM_{2.5}$ is severe in the winter, especially in January, while the O_3 is severe in the summer, especially in July and August [54].

Figure 2 Monthly average relative humidity and wind speed throughout the year.

3.2. Experimental setup

This experiment site was an office building located in the Jiangjin District in Chongqing. The roof top heat flux, temperatures (plant, roof top and bottom, and indoor air), soil temperature and humidity, and air conditioning (cooling + heating) energy consumption were compared over the course of the 12 months between September 2014 and September 2015 in three top-floor rooms that had identical orientation, floor area, function, and air conditioning system. All three rooms used the same split-system direct expansion air-source heat pump, which is typical in China and Europe. During the cooling season (Sept. 2014, Jun.–Sept. 2015) and the heating season (Nov. 2014–Feb. 2015), the air-source heat pump was turned on between 08:00 and 18:00 on workdays and turned off on the weekends. During the transitional season (Oct. 2014–May 2015, and Oct. 2015), the air conditioner was turned off all the time.

The energy consumption of the white and sedum-tray garden roofs during the cooling and heating seasons were computed via the energy meter. The seasonal and annual site energy savings, source energy savings, energy cost savings, and emission reductions were calculated using local source-to-site energy ratios, energy prices, and emissions factors.

3.3. Construction of the case study

In the three-story unoccupied office building in the Jiangjin District of Chongqing (106.44 °E, 29.49 °N), each tested room was 5.92 m × 3.62 m × 3.30 m and had an area of 21.4 m^2 (Figure 3a). According to the *Technical Specification for Planted Roofs (JGJ155-2013)*, Sedum *lineare* (carpet sedum or stonecrop) is an excellent drought-resistant and pulpy groundcover species widely distributed in Chongqing [54], which can replace the traditional insulation layer with the use of soilless cultivation. Sedum lineare thunb (needle stonecrop or carpet sedum) planting modules were applied to the roof section over room A on the top floor of the building. The properties of the modules are detailed in Table 1. The sedum-tray garden roof was designed according to the *Roofing Construction Technical Specification* (GB50345) [55]. Black coating was applied to the roof of room B, and highly reflective paint was applied to the roof of room C; the coating materials are shown in Table 2. The air-source heat pump for each room was turned on to measure the energy consumption or left off to measure the room air temperature reduction. The geometry, construction, air-source heat pump, and schedule for each room and its roof are detailed in Table 2.

Figure 3 (a) a three-dimensional model of the office building; (b) view of the black roof, white roof, and sedum-tray garden roof.

Figure 4 Figure 4 (a) sedum-tray module; and (b) installation of sensors.

Table 1 Description of Sedum lineare planting modules.

Table 2 Characteristics of the test rooms in the office building in the Jiangjin District of Chongqing.

3.4. Instrumentation and data acquisition

The measuring points were arranged according to the *Standard for Energy Efficiency Test of Public Buildings (JGJ/T177-2009)*. Sensors and data loggers were installed after their calibration and are detailed in Table 3. Exterior and interior surface temperatures, outside air and indoor air temperatures, roof surface heat flux, solar radiation, and electricity consumption were measured in each room 24 hours a day, with the data being recorded every five minutes. The details are shown in Table 3 and Figure 5.

Table 3 Measurement sensors and protocol in an office building in Jiangjin District, Chongqing.

Figure 5 Locations of temperature, heat flux, and roof reflectance sensors in the office building.

4. Results and discussion

Temperatures, heat flows, and energy uses were measured for a year in three side-by-side and similar rooms in a Chongqing office building. An analysis was performed to estimate the temperature reduction and thermal performance of representative summer and winter days. Furthermore, a comprehensive analysis of seasonal and annual temperature reductions, energy savings and emissions reductions are conducted. Additionally, comparative analysis of thermal performance after natural aging and peak-hour power demand reduction is also discussed. Finally, the influence of evaporation on the energy savings of sedum-tray garden roof is confirmed.

4.1. Representative summer and winter days

The dates of 22 September 2014 and 17 February 2015 were selected as representative sunny days in summer and winter, respectively. The maximum and minimum air temperatures on 22 Sept. 2014 were similar to the average maximum and minimum values on Sept 22nd between 2006 and 2014, and likewise for 17 Feb 2015 [57]. On the summer day, the outside air temperature ranged from 21.3 C (at 05:30 LST) to 36.8 C (15:10 LST); the global horizontal solar irradiance peaked at 0.774 KW/m^2 (12:45 LST), with 12.3 h from sunrise to sunset (Figure 6a). On the winter day, the outside air temperature ranged from 23.3 °C (at 16:45 LST) to 13.1 °C (07:50 LST); the global horizontal solar irradiance peaked at 0.65 kW/m^2 (13:05 LST), with 11.3 h from sunrise to sunset (Figure 6b).

Figure 6 Outside air temperature and global horizontal solar irradiance on (a) a sunny summer day (22 September 2014) and (b) a sunny winter day (12 2015).

4.2. Temperature reduction and thermal performance of the roofs

Figure 7 Roof top and roof bottom temperatures, roof top heat fluxes, indoor air temperatures, and daily cumulative AC energy consumption and temperature on (a–e) the summer day and (f–j) the winter day.

Table 4 Roof top and bottom temperatures and peak heat fluxes of rooms on the summer and winter days.

After correction for the heat flow through the interior walls, both sedum-tray garden roofs and white roofs demonstrated that they could lower the roof top and bottom temperatures and roof top heat flux, which could reduce air conditioning energy consumption in the summer, but increase energy consumption for heating in the winter. The heat flow of the white roof was from the outside to the interior in both summer and winter, but the heat flow of the sedum-tray garden roof was the opposite. The black and white roof tops were both exposed to the sunlight and atmosphere, with a wide range of temperatures, while the sedum-tray garden roof top was covered by plant modules and experienced more moderate temperature changes.

On the summer day, the roof top temperature and roof bottom temperature of room B reached their maxima at 14:30 and 18:40 LST, respectively; in room C, the corresponding maxima were attained 20 and 25 min later, respectively; in room A, the corresponding maxima were attained 10 and 17 min after those for room B , respectively (Figure 7a, b). The maximum indoor air temperature in the room with the sedum-tray garden roof was 26 °C, which was 0.2–1.2 °C less than those of the rooms with white or black roofs (Figure 7d). Because the air conditioners in all three rooms were turned on, we attribute this difference in indoor air temperature to the thermostat performance, rather than to roof solar heat gain. Long-wave radiation resulted in the temperature descending in the white and black roof topped rooms on the summer night. The added insulation increased the heat resistance of the sedum-tray garden roof top; hence, room A's roof top and bottom temperatures were lower than those of other two rooms at night. Moreover, the reductions in the white roof's top and bottom temperatures were greater than those of the black roof because of high emissivity. Normalized by roof area, the air conditioners in rooms C and A consumed 181.2 Wh/m^2 and 181.1 Wh/m^2 less electricity, respectively, than that in room B, both for a daily savings of approximately 45.6 % (Figure 7e). Therefore, the white and sedum-tray garden roofs had the same effect upon energy savings in the summer.

On the winter day, the roof top and bottom temperatures of room B reached their maxima at 14:40 and 18:00 LST, respectively; in room C, the corresponding maxima were attained 20 min later, and 10 min earlier, while in room A, the corresponding maxima were both attained 15 min earlier (Figure 7f, g). The maximal indoor air temperature in room A was 30 °C, which was slightly higher than those of rooms B and C, and the temperature reduction of the black roof after 12:00 was greater than that of the white roof, which experienced a rise in its indoor air temperature (Figure 7i). The roof bottom temperature showed a wave vibration pattern because the hot air from the air-conditioning (heating) unit's intermittent operation affected the temperature sensor in real time (Figure 7i). Plants withering and severe weather resulted in the roof bottom and indoor air temperatures of room A being mostly lower than those of other two rooms. Normalized by roof area, the air conditioners in room C and room A consumed approximately 57.5 Wh/m^2·day and 87.9 Wh/m^2·day more electricity than that in room B, for a daily savings of approximately −26.8 % and −17.5 %, respectively (Figure 7j). This result demonstrates that both the sedum-tray garden roofs and the white roofs had negative effects on the insulation of the top floor rooms, with the sedum-tray garden roof being worse.

4.3. Seasonal and annual temperature reductions, energy savings, and emissions reductions

Figure 8 presents the daily maximum and mean roof top, roof bottom, and indoor air temperatures. After being corrected for interior heat transfer, the seasonal mean reductions (black−garden) in the roof top, roof bottom, and indoor temperatures during the cooling season were approximately 14.8 °C, 8.7 °C, and 3.2 °C, respectively, and were roughly 1.8 times those of the white roof. During the heating season, the seasonal mean reduction (black−garden) in the roof top temperature was 3.5 °C greater than that of the white roof, but the roof bottom and indoor temperature reductions were approximately 1.4 °C and 1.2 °C, roughly half those of the white roof, meaning that the thermal performance of the room with the sedum-tray garden roof was better than that of the room with the white roof. Based on the above theoretical analysis, together with Eqs. (10), (11), (12), and (13), the seasonal and annual energy savings, corrected for the heat flow through the interior walls, and the emission reductions due to the white roof and sedum-tray garden roof are evaluated as follows.

Figure 8 Daily indoor air maximum and mean temperatures: (a) roof top, (b) roof bottom, and (c) indoor air.

Figure 9 Daily energy savings per unit of conditioned roof area during the heating season (a) and cooling season (b).

Figure 9 shows the daily energy savings per unit conditioned roof area of the white and sedum-tray garden roofs during the cooling and heating seasons. The seasonal cooling energy savings for the white and sedum-tray garden roofs were 4.8 kWh/m^2 and 5.7 kWh/m^2, respectively. The seasonal heating energy consumption of room A (sedum-tray garden roof) and room C (white roof) were 3.2 kWh/m^2 and 0.9 kWh/m^2 greater, respectively, than that of room B (black roof). Similarly, Su Bin [58] presented a study in Guangzhou showing that the power demand of rooms tested with green and cool roofs increased by 0.040 $kWh/m^2{\cdot}d$ and 0.020 $kWh/m^2{\cdot}d$, respectively, in the winter. Although both the white and sedum-tray garden roofs did not save energy during the winter, their annual energy savings were 3.9 kWh/m^2 and 2.5 kWh/m^2, respectively.

The seasonal (cooling and heating seasons) and annual mean values of energy consumption, energy cost savings, and emissions reductions (black−white and black−garden) are detailed in Table 5.

Table 5 Seasonal and annual mean values of energy savings and emission reduction.

4.4. Comparative analysis of thermal performance after natural aging

Days with meteorological conditions similar to the original test days were selected (2014-7-17 to 19 and 2015-7-17 to 19) in 2014 and 2015 to investigate the thermal performance of the white and sedum-tray garden roofs after one year of natural aging. Figure 10 shows the outdoor solar irradiation and air temperature on these days. In 2014, the mean outdoor air temperature was 30.7 °C, and the mean daily solar insolation was 23.6 $MJ/m^2 \cdot d$; in 2015, the mean outdoor air temperature was 31.7 °C, and the mean daily solar insolation was 22.6 $MJ/m^2 \cdot d$. In Sept. 2014 and Sept. 2015, the albedo of the white roof was measured using a TBQ-8 reflectance sensor, which is set on the open space of roofs and installed 1.5 m high from roofs, yielding values of 0.82 and 0.58, respectively, representing a 28.7 % decrease in one year. TBQ-8 reflectance sensor is composed of two solar reflectance sensors, one measures the total solar radiation and the other measures the solar reflectance reflected by roof, the albedo is the ratio of the reflected solar radiation to the total solar radiation. The data was measured in each room 24 hours a day over the course of the 12 months between September 2014 and September 2015 on three roofs, with the data being recorded every five minutes.

Figure 10 Outdoor solar irradiation and air temperature.

Figure 11 Temperature distributions of roofs (a, b); and indoor air temperature (c, d).

Table 6 Roof top and bottom temperature reductions in 2014 and 2015.

The indoor and outdoor temperature distributions of the three rooms are presented in Figure 11; the roof top and bottom temperatures during the conditioned hours and the indoor air temperature during the unconditioned hours were affected positively relative to the outdoor meteorological parameters. As illustrated in Figure 11, the roof bottom temperatures of the black roof in 2014 and 2015 reached their maxima at 19:15 LST and 19:10 LST, respectively; in room A, the corresponding maxima were attained 600 min later, on both July days, while the corresponding maxima in the room with white roof were attained 15 min later in 2014 and just 5 min later in 2015, as compared with room B. Table 6 shows the roof top and bottom temperature reductions before and after natural aging; the maximum and mean temperature reduction of the white roof top and bottom in 2015 were 12.0 °C and 5.2 °C and in 2014 were 5.2°C and 3.3°C, respectively. During the unconditioned hours (18:00 to 08:00 the next day), indoor mean air temperature quantity comes from temperature difference between black – garden were 2.5 °C and 2.7 °C on both July days, while those between black – white were 2.7 °C in 2014 and just 0.4 °C in 2015. Thus, the cooling performance of the white roof was significantly reduced after one year of natural aging.

Figure 12 Heat fluxes through the exterior surfaces of the roofs.

The heat fluxes through the exterior surfaces of the roofs at the time of installation and one year later are shown in Figure 12. In 2014, the peak heat flux of the black roof was 232 W/m^2, more than that of the white roof by 99 W/m^2; the heat flux of the black roof was 229.3 W/m^2 in 2015, just 11.7 W/m^2 less than the prior year. The heat flux of the sedum-tray garden roof was between −24 and −37 W/m^2 in 2014 and 2015, respectively.

Figure 11 illustrates that the meteorological conditions were similar on these two July days, but the black−white temperature difference was much smaller and the delay time was reduced by 10 min after a year of natural aging. Figure 11 demonstrates that the maximal white roof top temperature greatly increased, by 10 °C, from 2014 to 2015; thus, the cooling effect of the white roof, which was due to its reflectance, generally weakened after natural aging, causing the coated surface temperature to increase, and, consequently, the heat transmittance to become greater. After the year of natural aging, the white roof had become soiled and lost much of its solar reflectance.

This could result from (a) heavily polluted air; (b) poor performance of the white coating (some white coatings soil much more easily than others, depending on their chemistry); and/or (c) poor drainage from the roof (water ponding promotes soiling). By contrast, the insulation performance of the sedum-tray garden roof was maintained due to the life cycle of the plants.

4.5. Peak-hour power demand reduction

Figure 13 Daily values of the peak-hour cooling power demand reduction.

Figure 13 shows the daily values of the peak-hour cooling power demand reduction, calculated on each weekday during the cooling season (May through September) as the mean value of the roof power demand reduction from 08:00 to 12:00 and 19:00 to 23:00, LST. Based on the seasonal mean demand reduction, as calculated by Eqs. (10), (11), and (12), the peak-hour cooling power demand reduction of room C (4.60 W/m^2) was much greater than that calculated for room A (0.78 W/m^2). The peak-hour power demand reduction is an indicator for demand-side management. The result indicated the white roof performed better in enhancing the efficiency of the electrical terminal, reducing or postponing capital investments for units, and improving the quality of electrical services.

4.6. The influence of evaporation on the energy savings of the sedum-tray garden roof

Figure 14 Energy savings ratio and evaporation of the sedum-tray garden roof.

Heat loss through evaporation is the primary mechanism by which a sedum-tray garden roof cools and reduces heat flux [25] [26] [27]. Water evaporation was analyzed through the real-time monitoring of the weight changes of the planting modules; how the trend of the energy saving ratio varied with the water evaporation of the planting modules during air-conditioning is presented in Figure 14. As illustrated, the maximum and minimum evaporation rates were 2.01 kg/m^3 and −1.13 kg/m^3, which occurred on August 12 and July 13, and the energy savings ratio also reached its maximum and minimum concurrently. The energy saving ratio of the sedum-tray garden roof correlated with the tendency of evaporation; therefore, evaporation has a significant effect on the energy savings of the sedum-tray garden roof.

4.7. Summing up

In summer, both the white and sedum-tray garden roof decreased the heat gain through the roof, and reduced the cooling loads of rooms A and C during the air-conditioned hours and the indoor air temperature during the unconditioned hours. The roof top maximum temperatures of the sedum-tray garden and white roofs were 33.9 °C and 7.5 °C lower, respectively, than the black roof; the roof bottom maximum temperatures were 12.4 °C and 2.8 °C lower, respectively; the heat flows were 319 W/m^2 and 26 W/m^2 less, respectively; and, the indoor air temperatures were 2.1 °C and 0.4 °C lower, respectively, during the unconditioned hours. After correction for heat flow through the interior walls, the daily cooling energy consumptions of the rooms with the sedum-tray garden and white roofs were 25.0 % and 20.5 % lower, respectively, than that of the room with the black roof, and the daily cooling energy savings yielded by the sedum-tray garden roof (0.106 kWh/m^2·d) was 21.8 % greater than that from the white roof (0.087 kWh/m^2·d). The sedum-tray garden roof demonstrated better thermal performance and greater energy savings because the thermal properties of the sedum-tray garden roof were significantly affected by evaporation, and the change in the energy savings ratio was positively correlated with evaporation. The maximum evaporation was 1.13 kg/m^3 under the strong solar radiation and high temperature, and the corresponding energy savings ratio reached its maximum, 27.2 %.

Because of the effects of one year of natural aging, the reflectance of the white roof decreased by 23.6 %, to 0.58, causing its thermal performance to worsen and the power saving ratio to reduce. After natural aging, the roof top and bottom temperature difference and the maximum and mean temperature reduction of the white roof top and bottom in 2015 were 12.0 °C, 5.2 °C, 5.2 °C, and 3.3 C lower than in 2014, respectively. Also, the cooling energy consumption in 2014 was 0.033 kWh/m^2·d lower than that in 2015. The roof bottom temperature reached its maximum 10 min earlier in 2015 than in 2014. In contrast, the thermal performance and energy savings of the sedum-tray garden roof remained consistent between 2014 and 2015.

In winter, both the sedum-tray garden and white roofs have a negative effect on the insulation performance and energy savings of the building. The roof top maximum temperatures of the sedum-tray garden and white roofs were 14.2 °C and 4.0 °C lower, respectively, than that of the black roof;

the roof bottom maximum temperatures were 1.7 °C and 1.2 °C lower, respectively, the heat flows were 152 W/m^2 and 16 W/m^2 lower, respectively, and the indoor air temperatures were 0.3 °C and 1.8 °C lower, respectively, during the unconditioned hours. After correction for the heat flow through the interior walls, the daily cooling energy consumption of the rooms with the sedum-tray garden and white roofs were −9.9 % and −2.7 % lower, respectively, than that of the room with the black roof, and the daily cooling energy savings yielded by the sedum-tray garden roof (0.046 kW·h/m^2·d) was 2.8 times greater than that of the white roof (0.012 kW·h/m^2·d). The results for the white roof in winter agree with other researchers, but there are also deviations regarding the sedum-tray garden roof. Wang N [55] identified that a green roof could save energy depending on the plant canopy and thickness of the soil layer, while Santamouris concluded that a green roof had no influence during winter [33], and similar results were found of Jim C [60]. Except for the roof bottom temperature, the temperatures of the sedum-tray garden roof were lower than those of the white roof in both winter and summer. This indicates that the thermal performance of the sedum-tray garden roof is poor in winter. There are three possible reasons for this observation: 1) when air flowed through the weep holes, and water remained below the planting module, the natural convective heat transfers and rapid evaporation takes the heat away; 2) Chongqing experiences high amounts of precipitation in the winter and the air temperature is very low, so the insulation of the soil substrate is limited compared with the evaporative heat loss; and/or 3) Sedum *lineare* was hardy and resistant to the low temperatures such that the influence of plant transpiration exceeded the insulation supplied by the soil.

5. Conclusions

This paper summarized a study of sedum-tray garden roofs and white roofs that analyzed the heat transfer mechanisms of the roof tops and referenced the IPMVP for calculating and comparing the thermal performance and energy savings of three kinds of roofs on an office building under both air-conditioned and unconditioned conditions in Chongqing. The annual temperature distributions of the roofs, and the heat flux, evaporation, and indoor air temperature of the tested rooms were presented. Finally, based on the analyses of the annual energy savings, cost savings, annual carbon emission savings, and peak power demand reduction, the following conclusions can be drawn:

1) In summer (June–September), both the sedum-tray garden roof and white roofs could decrease the heat gain from the outside and lower the roof top and bottom temperatures and indoor air temperature, and reduce the cooling energy consumption. Compared with room B (black roof), room A (sedum-tray garden roof) and room C (white roof) reduced the air-conditioning daily energy consumption by 0.106 $kWh/m^2 \cdot d$ and 0.087 $kWh/m^2 \cdot d$, respectively, for average power saving rates of 25.0 % and 20.5 %, respectively. On days with similar meteorological conditions during the 2014 and 2015 cooling seasons, the black−white temperature difference was much smaller and the delay time was reduced by 10 min after a year. The white roof had a reflectance of 0.58 after the year of natural aging, which worsened the insulation performance and reduced the power savings by 0.033 $kWh/m^2 \cdot d$; in contrast, the thermal performance and energy savings of the sedum-tray garden roof maintained because of the life cycle of the plants.

2) In winter (November–February), both the sedum-tray garden roofs and white roofs increased the heat loss from the interior, and lowered the roof top and bottom temperature and the indoor air temperature, thus increasing the heating energy consumption. Compared to room B, rooms A and C reduced the air conditioning power consumption by 0.046 $kWh/m^2 \cdot d$ and 0.012 $kWh/m^2 \cdot d$, respectively, and the power saving rate by −9.9 % and −2.7 %, respectively.

3) Relative to the black roof, the white roof reduced the annual power consumption by 3.9 kWh/m^2, which was 1.6 times the energy savings for the sedum-tray garden roof; the annual energy saving ratio of the white roof was 7.99 %, and ratio of the white roof savings to the sedum-tray garden roof savings was 1.02. The annual conditioning-related energy cost savings of the white and sedum-tray garden roofs were 3.3 RMB/m^2 and 3.1 RMB/m^2, respectively. The annual CO_2, NOx, and SO_2 emission reductions of the white roof were 3.2 kg/m^2, 17.9 g/m^2, and 43.3 g/m^2, respectively, while those of the sedum-tray garden roof were 2.1 kg/m^2, 11.4 g/m^2, and 27.8 g/m^2, respectively. The peak-hour cooling power demand reduction of the white roof (1.06 W/m^2) was approximately 20 % higher than that of the sedum-tray garden roof (0.88 W/m^2). These findings imply that the energy savings due to the white roof were greater than those for the sedum-tray garden roof.

Summer rainfall patterns, climate, energy prices, and storm water management fees and policies may greatly influence the results of the comparison. The observed energy savings were not all as expected, but it has become common for people to not opt for dark roofs that increase the building's energy costs, summer urban heat islands, and global warming.

Acknowledgments

This research work was supported by the China National Key R&D Program (No. 2017YFC0702903), Chongqing City Fundamental and Advanced Research Projects (No. CSTC2014jcyjA90018), and the National Natural Science Foundation of China (No. 51578086).

Reference

[1] Cotana F, Rossi F, Filipponi M., Coccia V., Pisello A.L., Bonamente E., Petrozzi A., Cavalaglio G. Albedo control as an effective strategy to tackle Global Warming: A case study. Appl Energy. 130 (2014) 641-647.

[2] Sproul J., Wan M.P., Mandel B.H., Rosenfel A.H.. Economic comparison of white, green, and black flat roofs in the United States. Energy Build 71(2014) 20-27.

[3] Tong S., Li H. An efficient model development and experimental study for the heat transfer in naturally ventilated inclined roofs. Build Environ 81(2014) 296-308.

[4] He Y, Yu H, Dong N, Ye, H. Thermal and energy performance assessment of extensive green roof in summer: a case study of a lightweight building in shanghai. Energy Build 127(2016) 762-773.

[5] Xiao M., Lin Y., Han J., Zhang G. A review of green roof research and development in China. Renew Sustain Energy Rev 40(2014) 633-648.

[6] Oberndorfer E., Lundholm J., Bass B., Coffman R.R., Doshi H., Dunnett N., Gaffin S., Köhler M., Liu K.K.Y, Rowe B. Green roofs as urban ecosystems: ecological structures, functions, and services. Bioscience 57(2007) 823–33.

[7] Lazzrin R.M., Castellotti F, Busato F. Experimental measurements and numerical modelling of green roofs. Energy Build. 37 (2005) 1260-1267.

[8] Berardi U, Ghaffarianhoseini A, Ghaffarianhoseini A. State-of-the-art analysis of the environmental benefits of green roofs. Appl Energy 115(2014) 411–28.

[9] Berndtsson J.C. Green roof performance towards management of runoff water quantity and quality: a review. Ecol Eng 36(2014) 351–60.

[10] Rosado P.J, Faulkner D, Sullivan D.P, Levinson, R. Measured temperature reductions and energy savings from a cool tile roof on a central California home. Energy Build 80(2014) 57-71.

[11] Saadatian O, Sopian K, Salleh E, Lim CH, Riffat S, Saadatian E, Toudeshki A, Sulaiman M.Y. A review of energy aspects of green roofs. Renew Sustain Energy Rev 23(2013) 155–68.

[12] Coutts A.M, Daly E, Beringer J, Tapper N.J. Assessing practical measures to reduce urban heat: Green and cool roofs. Build Environ 70(2013) 266-276.

[13] Han L.L, Ke S.Z, Chen M.L, The Application of Container-type Green Roof in Ancient Architecture—Examples of the Green Roofs of CPPCC and NPC Buildings in Huangpu District of Shanghai. China Garden 31(2015) 9-12,

[14] Getter K.L, Rowe D.B, Robertson G.P, Cregg B.M, Andresen J.A. Carbon seques-tration potential of extensive green roofs. Environ Sci Technol 43(2009) 7564–70.

[15] Akbari H, Pomerantz M, Taha H. Cool surfaces and shade trees to reduce energy use and improve air quality in urban areas. Solar Energy 70(2001), 295-310.

[16] Synnefa A., Santamouris M., Akbari H. Estimating the effect of using cool coatings on energy loads and thermal comfort in residential buildings in various climatic conditions. Energy Build 39(2007) 1167-1174.

[17] Cotana F, Rossi F, Filipponi M, Coccia V, Pisello A.L, Bonamente E, Petrozzi A, Cavalaglio G. Albedo control as an effective strategy to tackle Global Warming: A case study. Appl Energy 130(2014) 641-647.

[18] Akbari H, Damon Matthews H, Seto D. The long-term effect of increasing the albedo of urban areas. Environmental Research Letters 7(2012) 24004-24013(10).

[19] Dornelles K, Caram R, Sichieri E. Natural Weathering of Cool Coatings and its Effect on Solar Reflectance of Roof Surfaces. Energy Procedia 78(2015) 1587-1592.

[20] Mastrapostoli E, Santamouris M, Kolokotsa D. On the ageing of cool roofs: Measure of the optical degradation, chemical and biological analysis and assessment of the energy impact. Energy Build 114(2016) 191-199.

[21] Zhuang C.Q. Natural aging processes of reflective roofs and its effects on energy consumption——a case study of a dormitory building in Xiamen. 2016 Doctoral dissertation, Chongqing university.

[22] Jiang W.H, Chen D.J. Analysis on the Air Quality and Pollution Characteristics in Chongqing Urban Area. Sichuan Environ 34(2015), 67-71.

[23] Coutts A.M, Daly E, Beringer J, Tapper N.J. Assessing practical measures to reduce urban heat: Green and cool roofs. Build Environ 70(2013) 266-276.

[24] Xu J.M, Contrastive research on energy savings from the application of reflective roof and green roof—a case study of typical office building in Chongqing. Chongqing University, 2014.

[25] Saadatian O, Sopian K, Salleh E, Lim C.H, Riffat S, Saadatian E, Toudeshki A, Sulaiman M.Y. A review of energy aspects of green roofs. Renew Sustain Energy Rev 23(2013) 155–68.

[26] Hashemi S.S.G, Mahmud H.B, Ashraf M.A. Performance of green roofs with respect to water quality and reduction of energy consumption in tropics: a review. Renew Sustain Energy Rev 52(2015) 669–79.

[27] Onmura S., Matsumoto M., Hokoi S. Study on evaporative cooling effect of roof lawn gardens. Energy Build 33(2001) 653-666.

[28] Ekaterini E, Dimitris A. The contribution of a planted roof to the thermal protection of buildings in Greece. Energy Build 27(1998) 29–36.

[29] Hao Y, Huo R. Introduction on part revised contents of technical code for roof engineering gb50345. Construction Technol 40(2013) 102-103.

[30] Razzaghmanesh M, Beecham S, Kazemi F. The growth and survival of plants in urban green roofs in a dry climate. Sci Total Environ 476-477(2014) 288–97.

[31] Wong N.H, Chen Y, Ong C.L, Sia A. Investigation of thermal benefits of roof top garden in the tropical environment. Build Environ 38(2003) 261–70.

[32] Zhao M, Srebric J. Assessment of green roof performance for sustainable buildings under winter weather conditions. Central South Univ 19(2012) 639–44.

[33] Santamouris M, Pavlou C, Doukas P, Mihalakakou G, Synnefa A, Hatzibiros A, Patargias P. Investigating and analyzing the energy and environment alperformance of an experimental green roof system installed in a nursery school building in Athens, Greece. Energy 32(2007) 1781-8.

[34] Jim C.Y, Tsang S.W. Biophysical properties and thermal performance of an intensive green roof. Build Environ 46(2011) 1263–74.

[35] Takebayashi H, Moriyama M. Surface heat budget on green roof and high reflection roof for mitigation of urban heat island. Build Environ 42(2007) 2971-9.

[36] Scherba A, Sailor D.J, Rosenstiel T.N, Wamser C.C. Modeling impacts of roof reflectivity, integrated photovoltaic panels and green roof systems on sensible heat flux into the urban environment. Build Environ 46(2011) 2542-51.

[37] Berndtsson J.C. Green roof performance towards management of runoff water quantity and quality: a review. Ecol Eng 36(2010) 351–60.

[38] Berndtsson J.C. Green roof performance towards management of runoff water quantity and quality: a review. Ecol Eng 36(2010) 351–60.

[39] Zhang X, Shen L, Tam V, Lee W. Barrier stoimplement extensive green roof systems: a Hong Kong study. Renew Sustain Energy Rev 16(2012) 314–9.

[40] Berndtsson J.C. Green roof performance towards management of runoff water quantity and quality: a review. Ecol Eng 36(2010) 351–60.

[41] Getter K.L, Rowe D.B, Robertson G.P, Cregg B.M, Andresen J.A. Carbon sequestration potential of extensite green roofs. Environ SciTechnol 43(2009) 7564–70.

[42] Gao Y, Xu J, Yang S, Tang X, Zhou Q, Ge J, Levinson R. Cool roofs in China: Policy review, building simulations, and proof-of-concept experiments. Energy Policy 74(2014) 190-214.

[43] Gao Y.F, Guo R, Ronnen L. Measured temperature reductions and energy savings from a white, garden flat roof in a Chongqing office building. 4th International Conference on Countermeasures to Urban Heat Island, 30-31 May and 1 June 2016, National University of Singapore, Singapore.

[44] Rosado P.J, Faulkner D, Sullivan D.P, Levinson R. Measured temperature reductions and energy savings from a cool tile roof on a central California home. Energy Build 80(2014) 57-71.

[45] Hendron R., Engebrecht C. United States DOE Building America House Simulation Protocols (Revised October 2010). U.S. DOE Build Technol Prog, 2010.

[46] Rosado P.J, Faulkner D, Sullivan D.P, Levinson R. Measured temperature reductions and energy savings from a cool tile roof on a central California home. Energy Build 80(2014) 57-71.

[47] International performance measurement and verification protocol. In: Concepts and Options for Determining Energy and Water Savings, DOE/GO-102002–1554, vol. 1. Washington, DC: Office of Energy Efficiency and Renewable Energy, US Department of Energy; March 2010.

[48] Ginestet S, Marchio D. Retro and on-going commissioning tool applied to an existing building: operability and results of ipmvp. Energy 35(2010) 1717-1723.

[49] International performance measurement and verification protocol. In: IPMVP Framework And Options, EVO 10000-1:2010, vol. 1: Concepts and Options for Determining Energy and Water Savings, US Department of Energy; March 2010.

[50] Zhu Y.X. Building environment. China Architecture & Building Press. 2013.

[51] Cai W, Wang C, Jin Z, Chen J. Quantifying baseline emission factors of air pollutants in china's regional power grids. Environ Sci Technol 47(2013) 3590.

[52] China regional power grid baseline emission factor [URL], 2015. http://cdm.ccchina.gov.cn

[53] CMPB, 2013. Chongqing power grid peak and valley load of electricity price, Chongqing Municipal Price Bureau.

[54] Liu Y.X, Fang W, Ma L.H. Investigation on Plant Resources of Jingtian Branch in Chongqing and Its Vertical Greening Advantages. Forestry Investigation and Planning 2013(6) 124-128.

[55] Wang S.H. Summary of the revision of the Technical Specification for Roofing Engineering (gb50345-2004). Build Technol 42(2011) 107-109.

[56] Zhang Q.Y, Yang H.X. Standard Meteorological Data Handbook for Buildings. China Construction Industry Press, 2012.

[57] The Chinese Weather Net, The Chongqing climate impact assessment, 2014, http://cq.weather.com.cn/qxfwcp/yqhpj/10/2206541.shtml.

[58] Su B. Green roof and cold roof energy saving and carbon reduction effect comparison. Chongqing University, 2016.

[59] Forchungsgesellschaft Landschaftsentwicklung Landschaftsbau e.V. (FLL),Guidelines for the planning, construction and maintenance of green roofing –Green Roofing Guideline, Germany, 2008.

[60] Jim C.Y, Tsang S.W. Biophysical properties and thermal performance of an intensive green roof. Build Environ 2011;46:1263–74.

Figure captions

Figure 1 Mean outside air temperature and global solar irradiance through the year.

Figure 2 Monthly average relative humidity and wind speed throughout the year.

Figure 3 (a) a three-dimensional model of the office building;
(b) view of the black roof, white roof, and sedum-tray garden roof.

Figure 4 (a) sedum-tray module; and (b) installation of sensors.

Figure 5: Figure 5 Locations of temperature, heat flux, and roof reflectance sensors in the office building.

Figure 6 Outside air temperature and global horizontal solar irradiance on (a) a sunny summer day (22 September 2014) and (b) a sunny winter day (12 January 2015).

Figure 7 Roof top and roof bottom temperatures, roof top heat fluxes, indoor air temperatures, and daily cumulative AC energy consumption and temperature on (a–e) the summer day and (f–j) the winter day.

Figure 8 Daily indoor air maximum and mean temperatures: (a) roof top, (b) roof bottom, and (c) indoor air.

Figure 9 Daily energy savings per unit of conditioned roof area during the heating season (a) and cooling season (b).

Figure 10 Outdoor solar irradiation and air temperature.

Figure 11 Figure 11 Temperature distributions of roofs (a, b); and indoor air temperature (c, d).

Figure 12 Heat fluxes through the exterior surfaces of the roofs.

Figure 13 Daily values of the peak-hour cooling power demand reduction.

Figure 14 Daily values of peak-hour cooling power demand reduction.

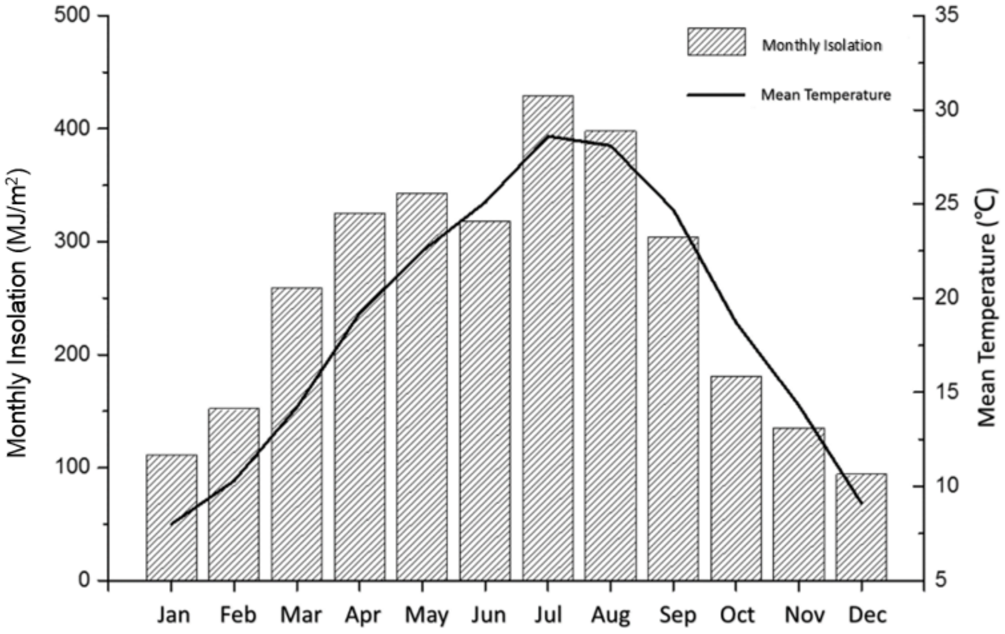

Figure 1 Mean outside air temperature and global solar irradiance through the year.

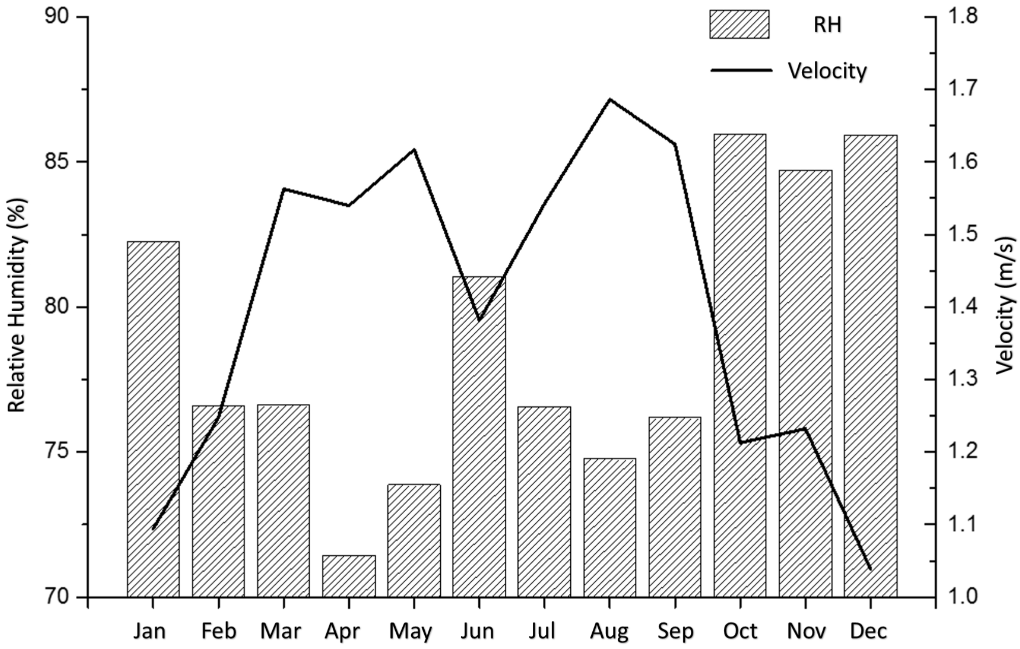

Figure 2 Monthly average relative humidity and wind speed throughout the year.

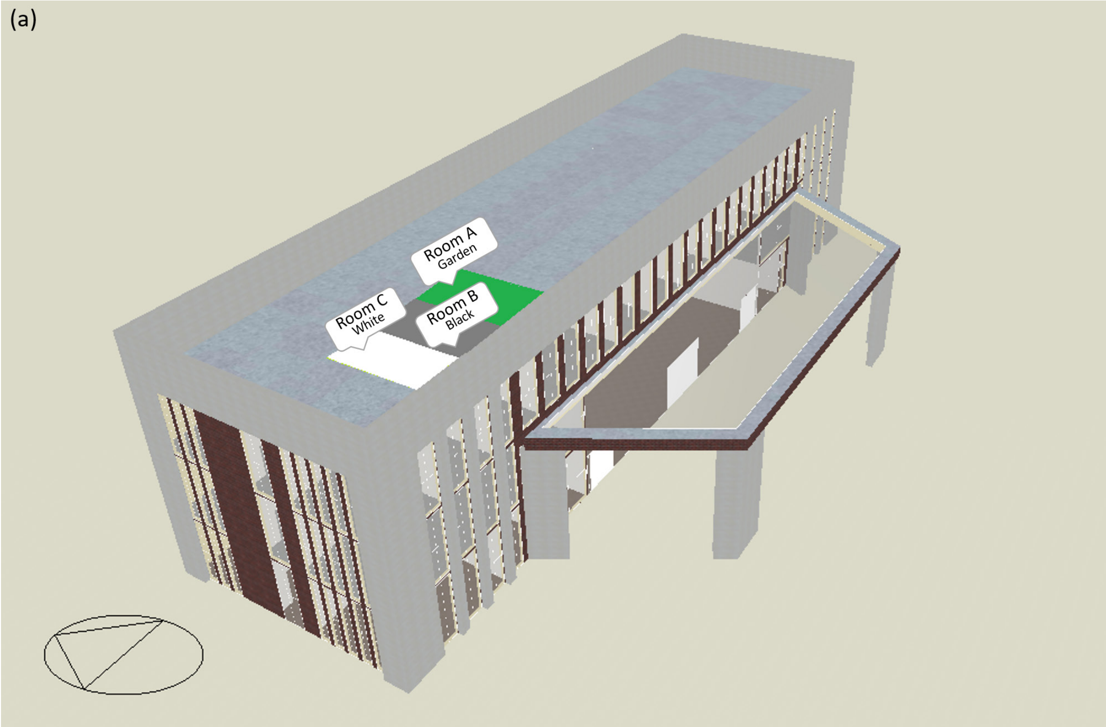

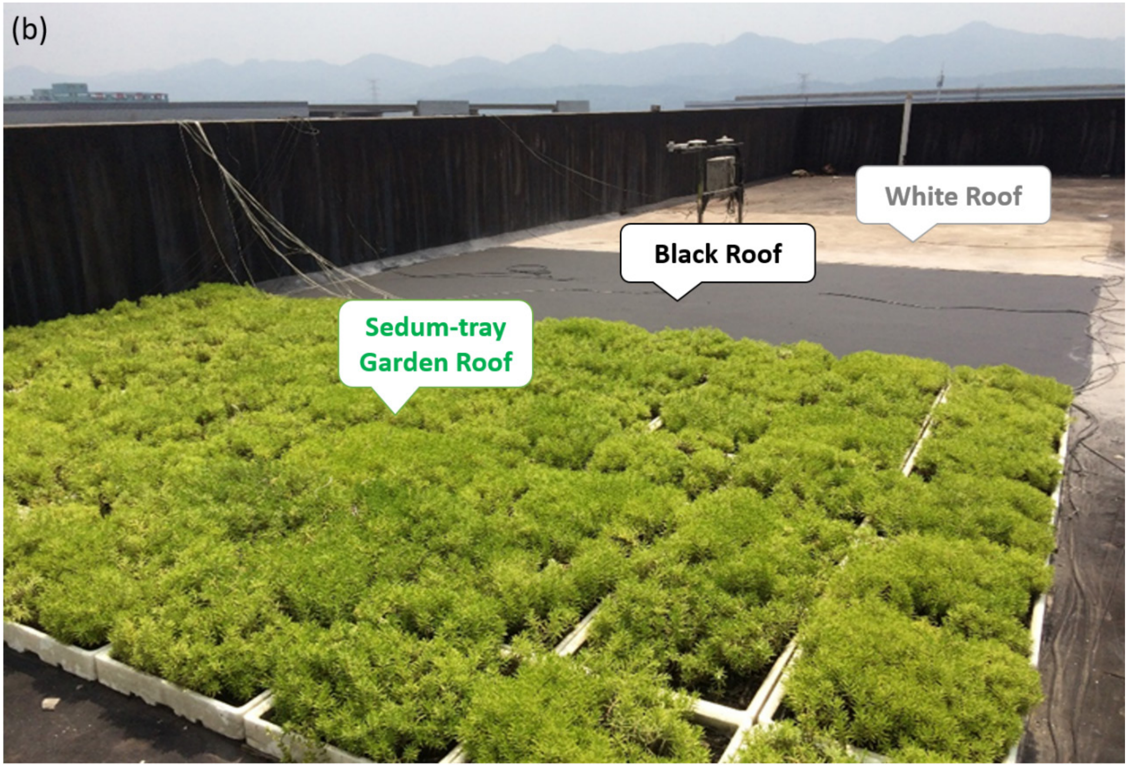

Figure 3 (a) three - dimensional model of the office building; (b) field for black roof, white roof and containered planting roof.

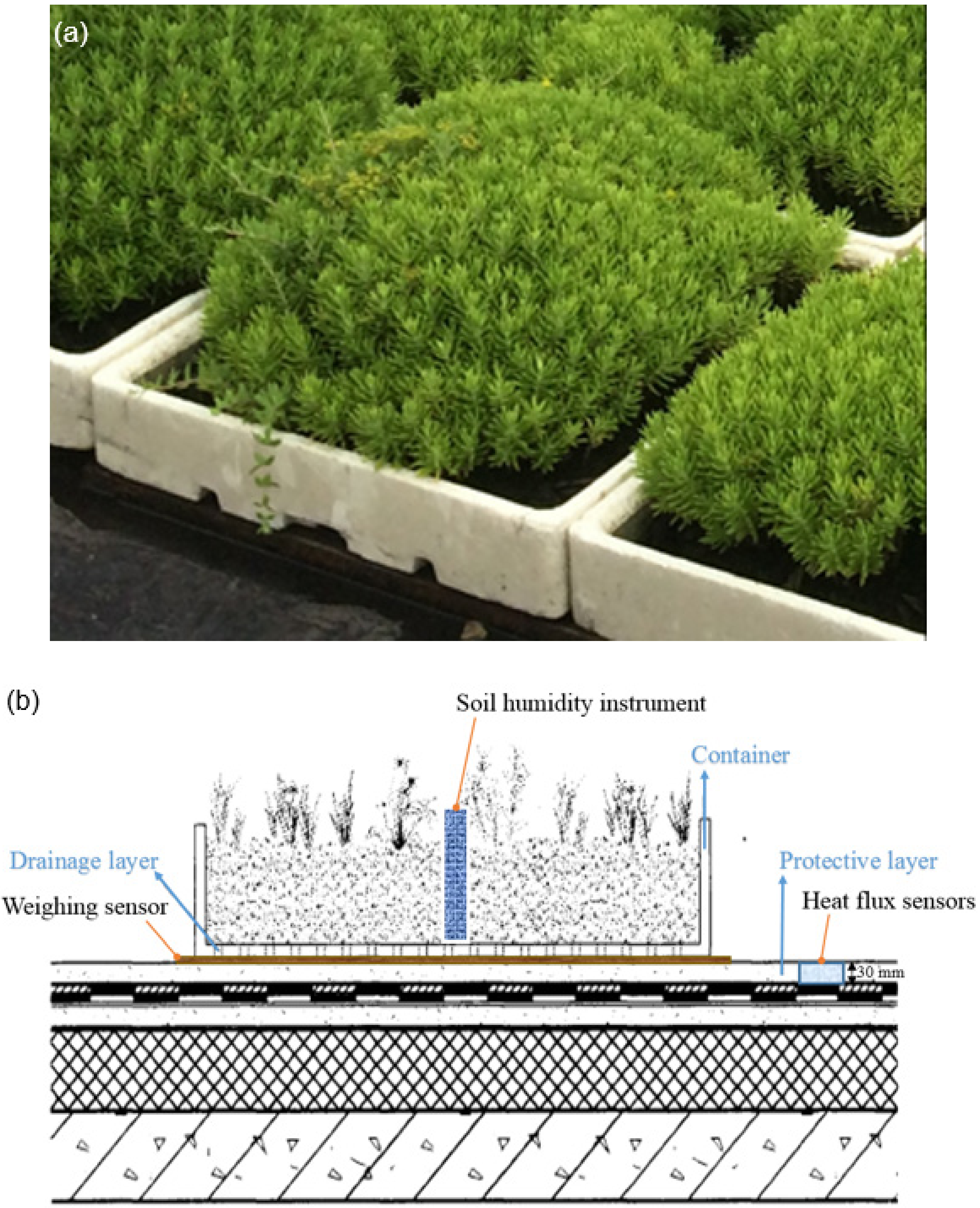

Figure 4 (a) sedum-tray module; and (b) installation of sensors

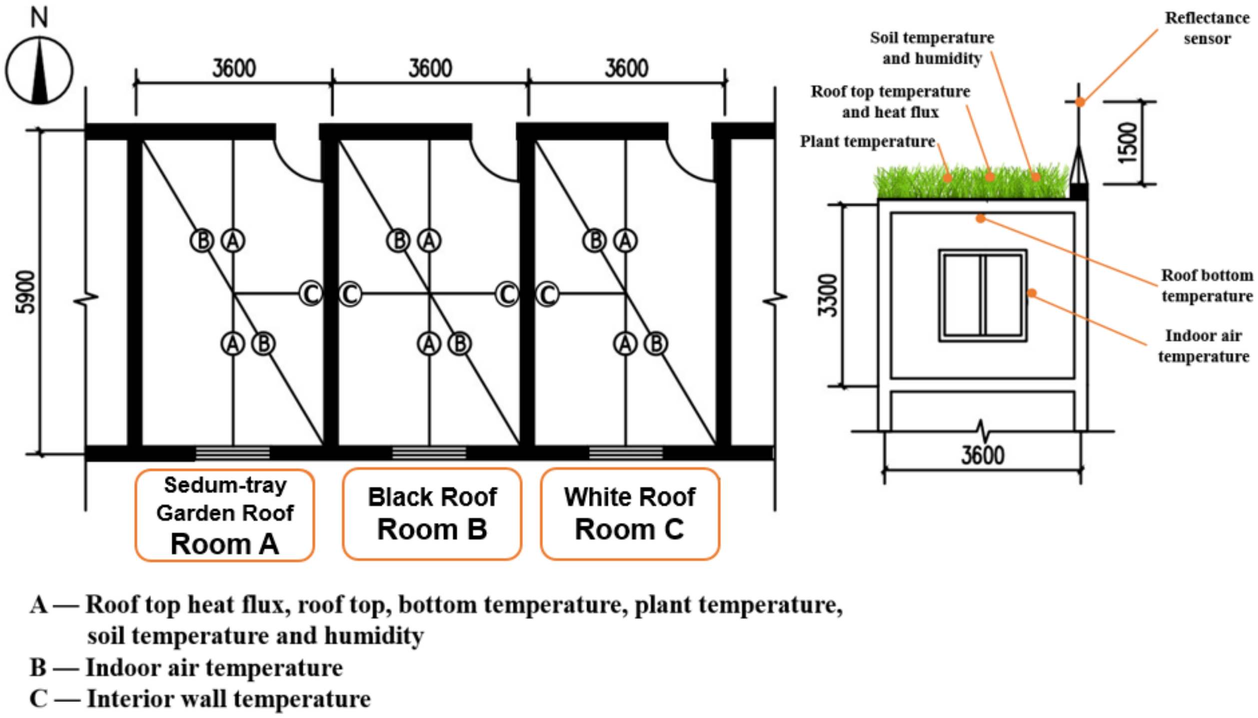

Figure 5 Locations of temperature, heat flux, and roof reflectance sensors in the office building.

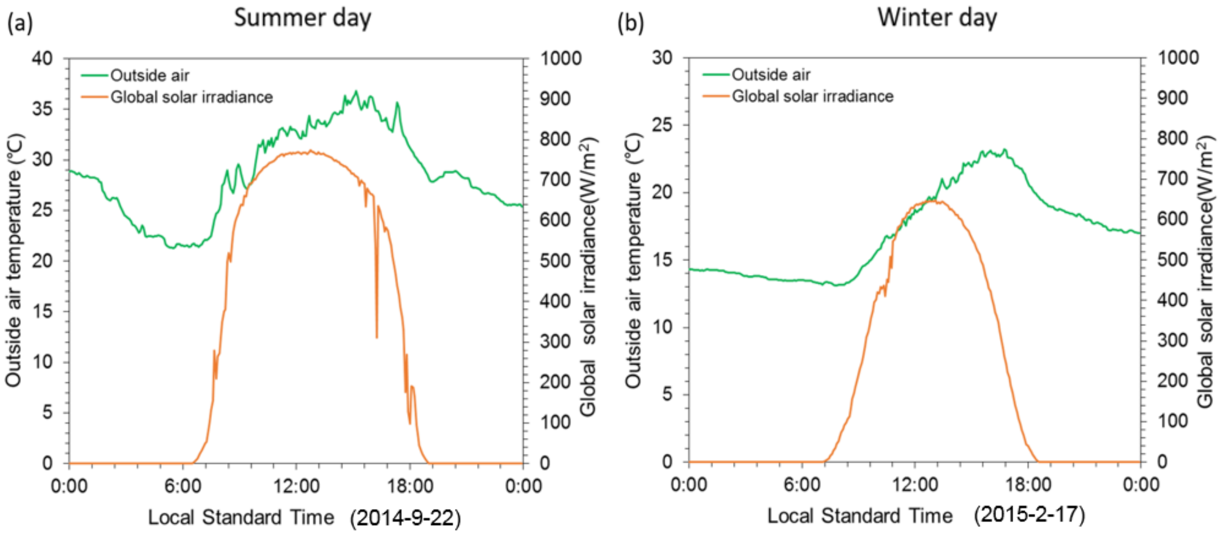

Figure 6 Outside air temperature and global horizontal solar irradiance on (a) a sunny summer day (22 September 2014) and (b) a sunny winter day (12 January 2015).

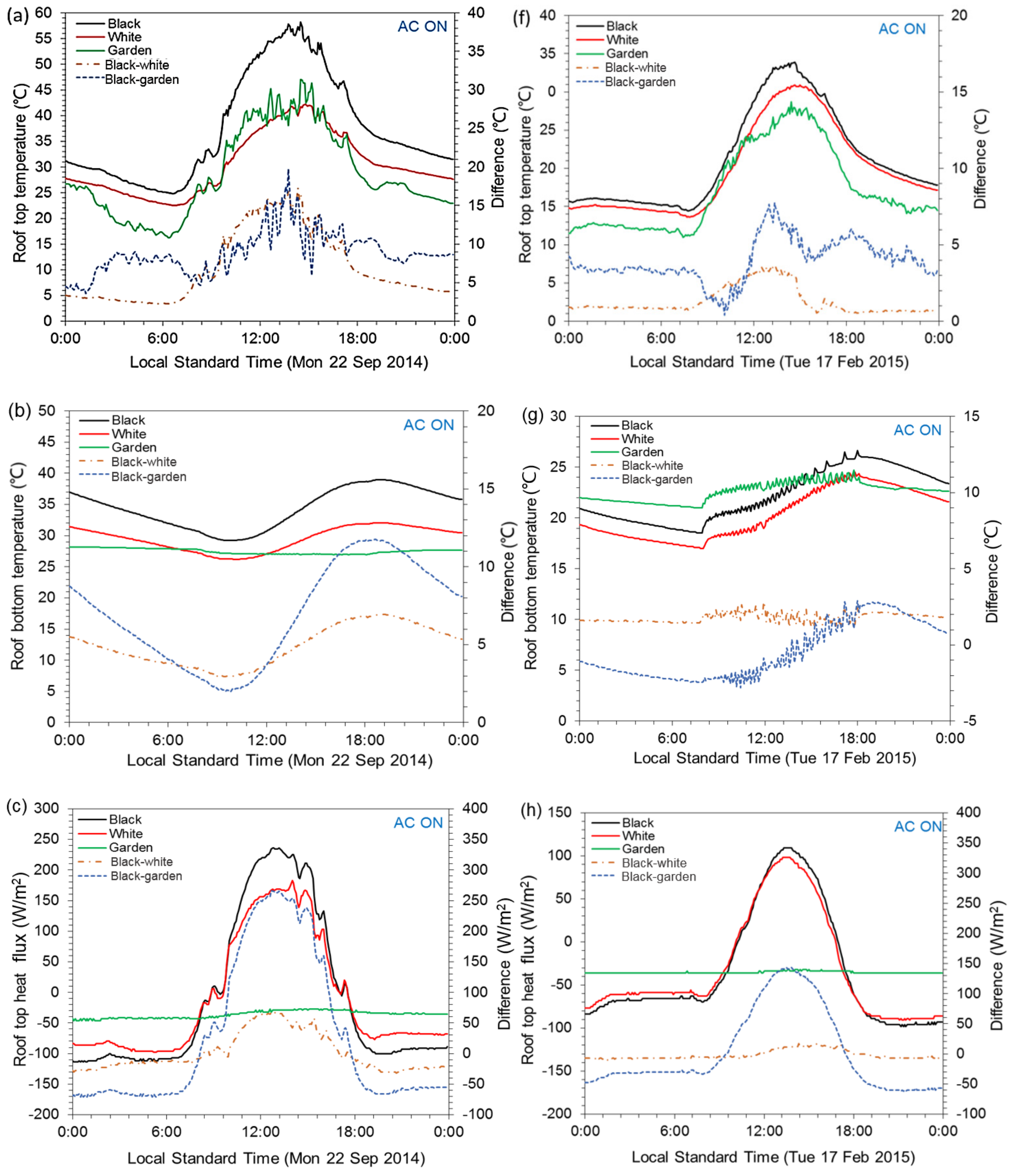
(a)
Black
White
Garden
Black-white
Black-garden
AC ON
Roof top temperature (°C)
Difference (°C)
0 5 10 15 20 25 30 35 40 45 50 55 60
0 5 10 15 20 25 30 35 40
0:00 6:00 12:00 18:00 0:00
Local Standard Time (Mon 22 Sep 2014)
(f)
Black
White
Garden
Black-white
Black-garden
AC ON
Roof top temperature (°C)
Difference (°C)
0 5 10 15 20 25 0 35 40
0 5 10 15 20
0:00 6:00 12:00 18:00 0:00
Local Standard Time (Tue 17 Feb 2015)
(b)
Black
White
Garden
Black-white
Black-garden
AC ON
Roof bottom temperature (°C)
Difference (°C)
0 5 10 15 20 25 30 35 40 45 50
0 5 10 15 20
0:00 6:00 12:00 18:00 0:00
Local Standard Time (Mon 22 Sep 2014)
(g)
Black
White
Garden
Black-white
Black-garden
AC ON
Roof bottom temperature (°C)
Difference (°C)
0 5 10 15 20 25 30
-5 0 5 10 15
0:00 6:00 12:00 18:00 0:00
Local Standard Time (Tue 17 Feb 2015)
(c)
Black
White
Garden
Black-white
Black-garden
AC ON
Roof top heat flux (W/m²)
Difference (W/m²)
-200 -150 -100 -50 0 50 100 150 200 250 300
-100 -50 0 50 100 150 200 250 300 350 400
0:00 6:00 12:00 18:00 0:00
Local Standard Time (Mon 22 Sep 2014)
(h)
Black
White
Garden
Black-white
Black-garden
AC ON
Roof top heat flux (W/m²)
Difference (W/m²)
-200 -150 -100 -50 0 50 100 150
-100 -50 0 50 100 150 200 250 300 350 400
0:00 6:00 12:00 18:00 0:00
Local Standard Time (Tue 17 Feb 2015)

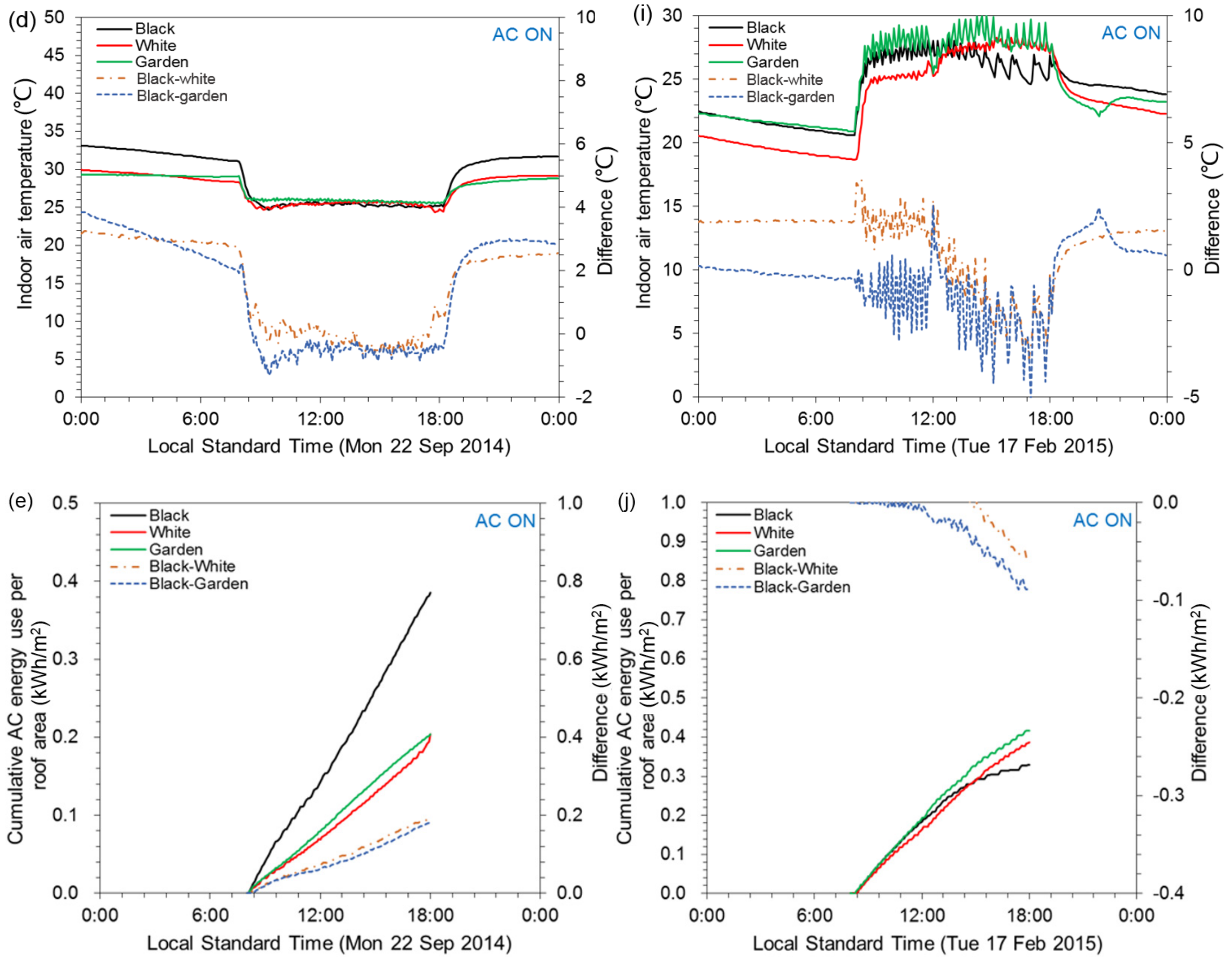

Figure 7 Roof top and roof bottom temperatures, roof top heat fluxes, indoor air temperatures, and daily cumulative AC energy consumption and temperature on (a–e) the summer day and (f–j) the winter day[1,2].

---

[1] "Garden" in the charts refers to the sedum-tray garden roof, the same below.

[2] "Black−White" and "Black−Garden" are the differences in temperature, heat flux, and energy consumption between the black roof and white roof and between the black roof and sedum-tray garden roof, respectively.

(a)

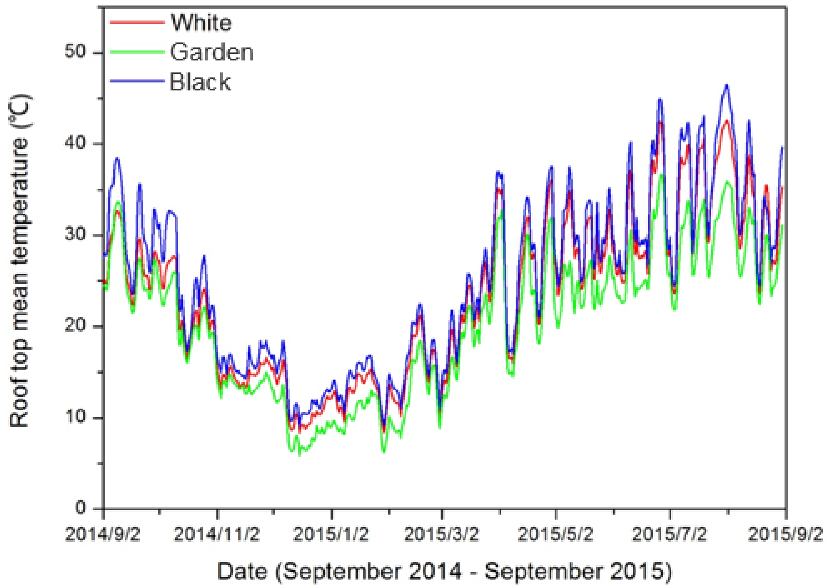
White
Garden
Black
Roof top mean temperature (℃)
0
10
20
30
40
50
2014/9/2
2014/11/2
2015/1/2
2015/3/2
2015/5/2
2015/7/2
2015/9/2
Date (September 2014 - September 2015)

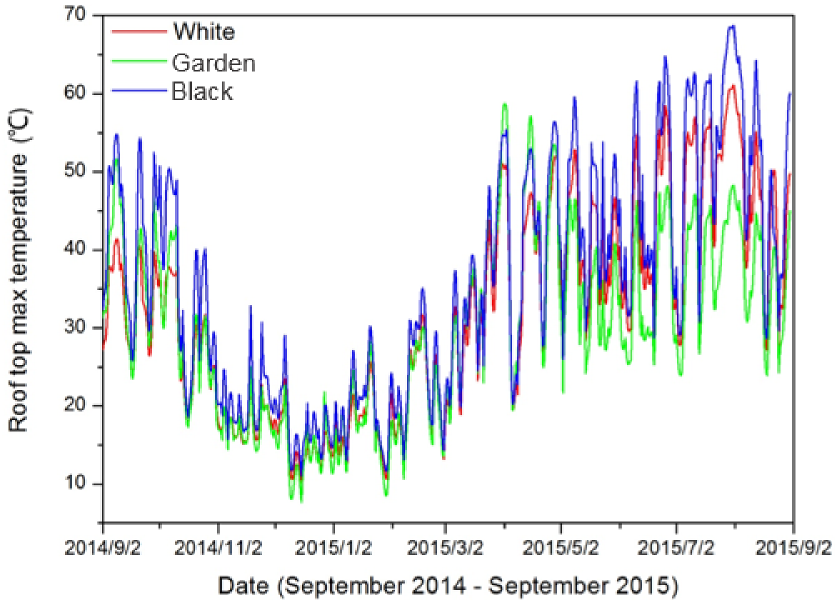
White
Garden
Black
Roof top max temperature (℃)
10
20
30
40
50
60
70
2014/9/2
2014/11/2
2015/1/2
2015/3/2
2015/5/2
2015/7/2
2015/9/2
Date (September 2014 - September 2015)

(b)

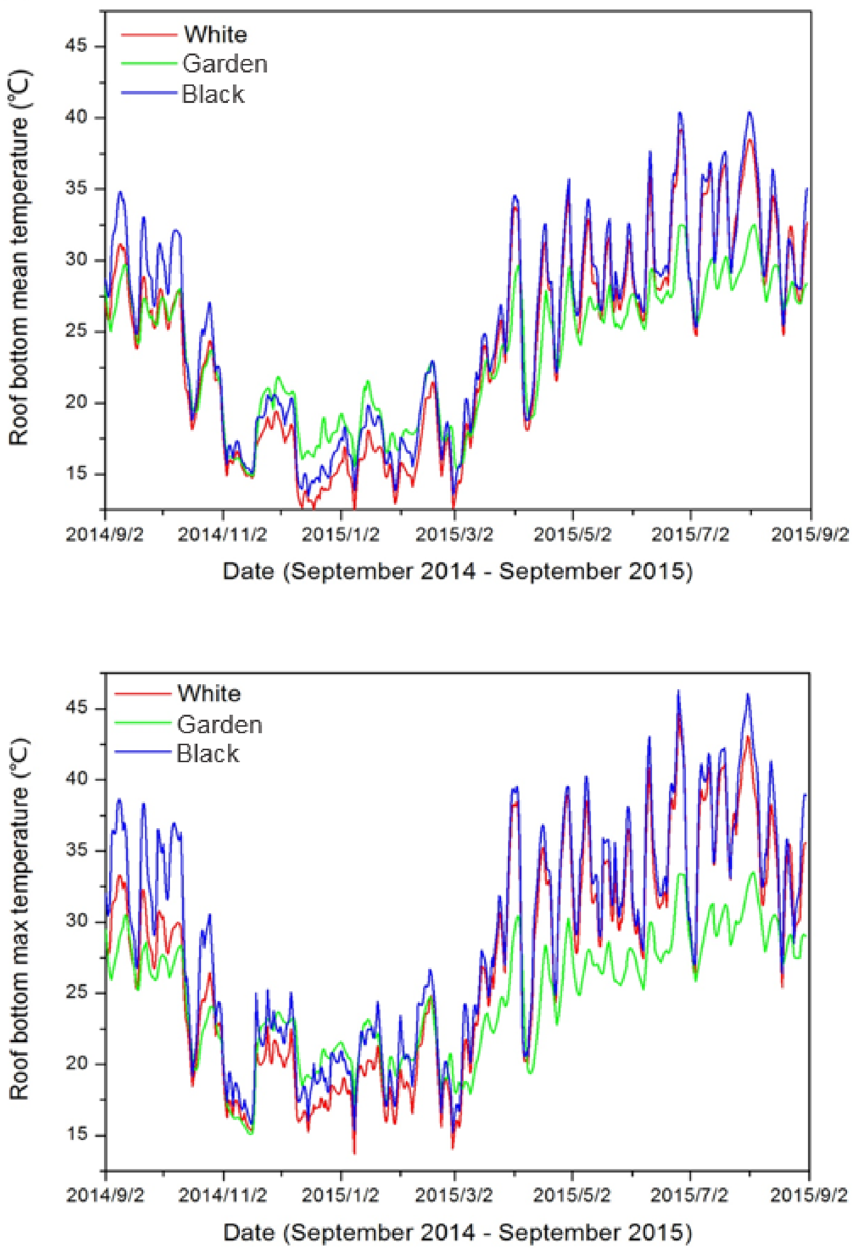
White
Garden
Black
Roof bottom mean temperature (°C)
45
40
35
30
25
20
15
2014/9/2
2014/11/2
2015/1/2
2015/3/2
2015/5/2
2015/7/2
2015/9/2
Date (September 2014 - September 2015)
White
Garden
Black
Roof bottom max temperature (°C)
45
40
35
30
25
20
15
2014/9/2
2014/11/2
2015/1/2
2015/3/2
2015/5/2
2015/7/2
2015/9/2
Date (September 2014 - September 2015)

(c)

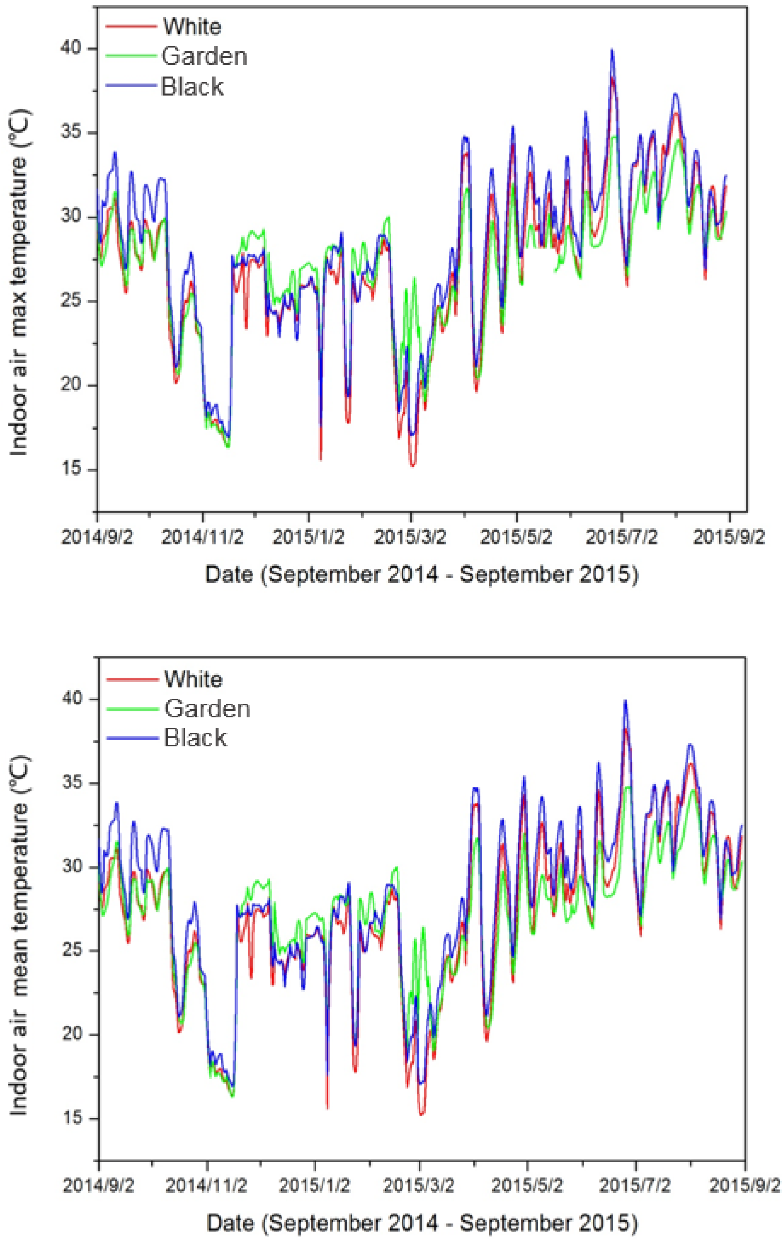

Figure 8 Daily indoor air maximum and mean temperatures: (a) roof top, (b) roof bottom, and (c) indoor air.

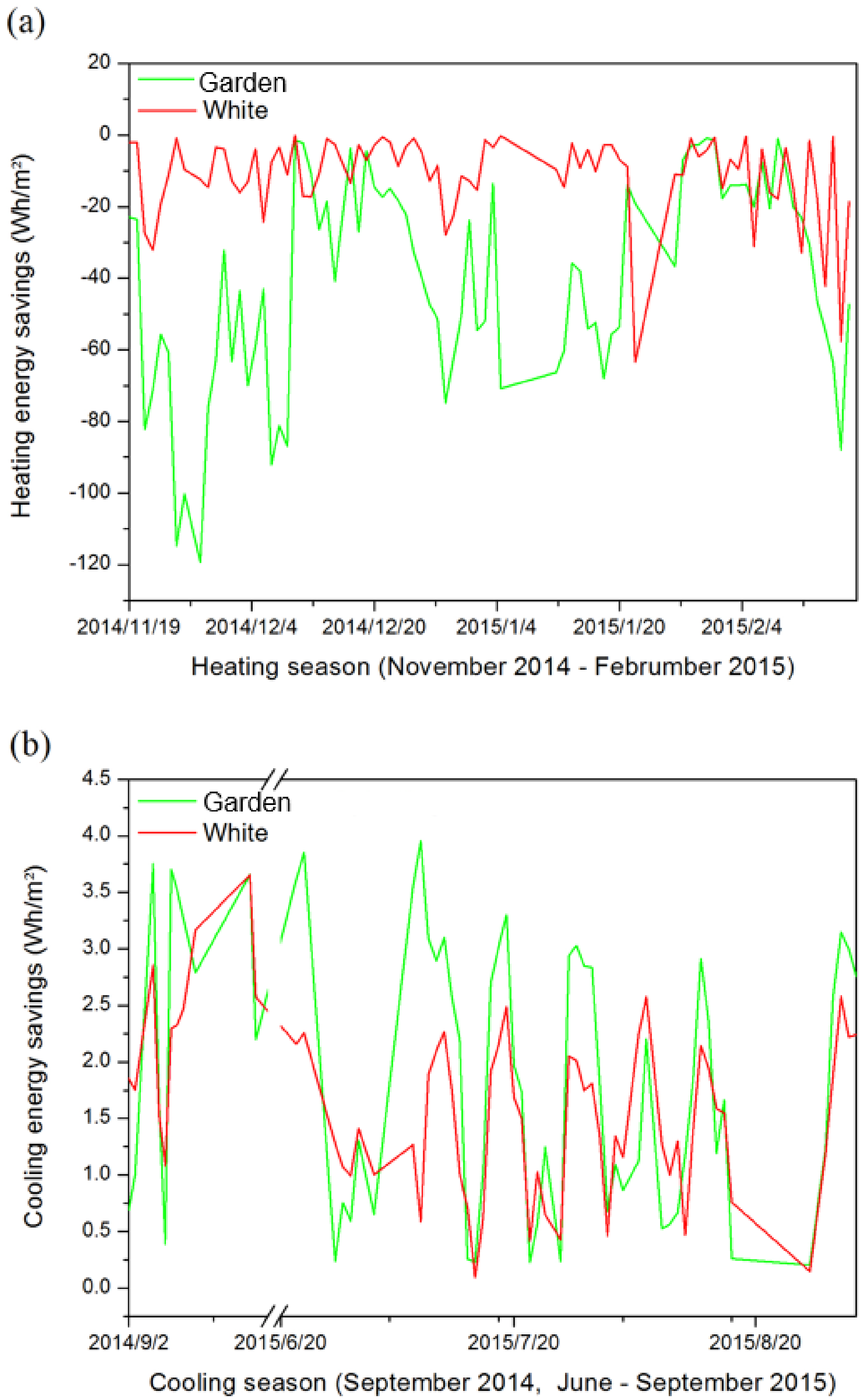

Figure 9 Daily energy savings per unit of conditioned roof area during the heating season (a) and cooling season (b).

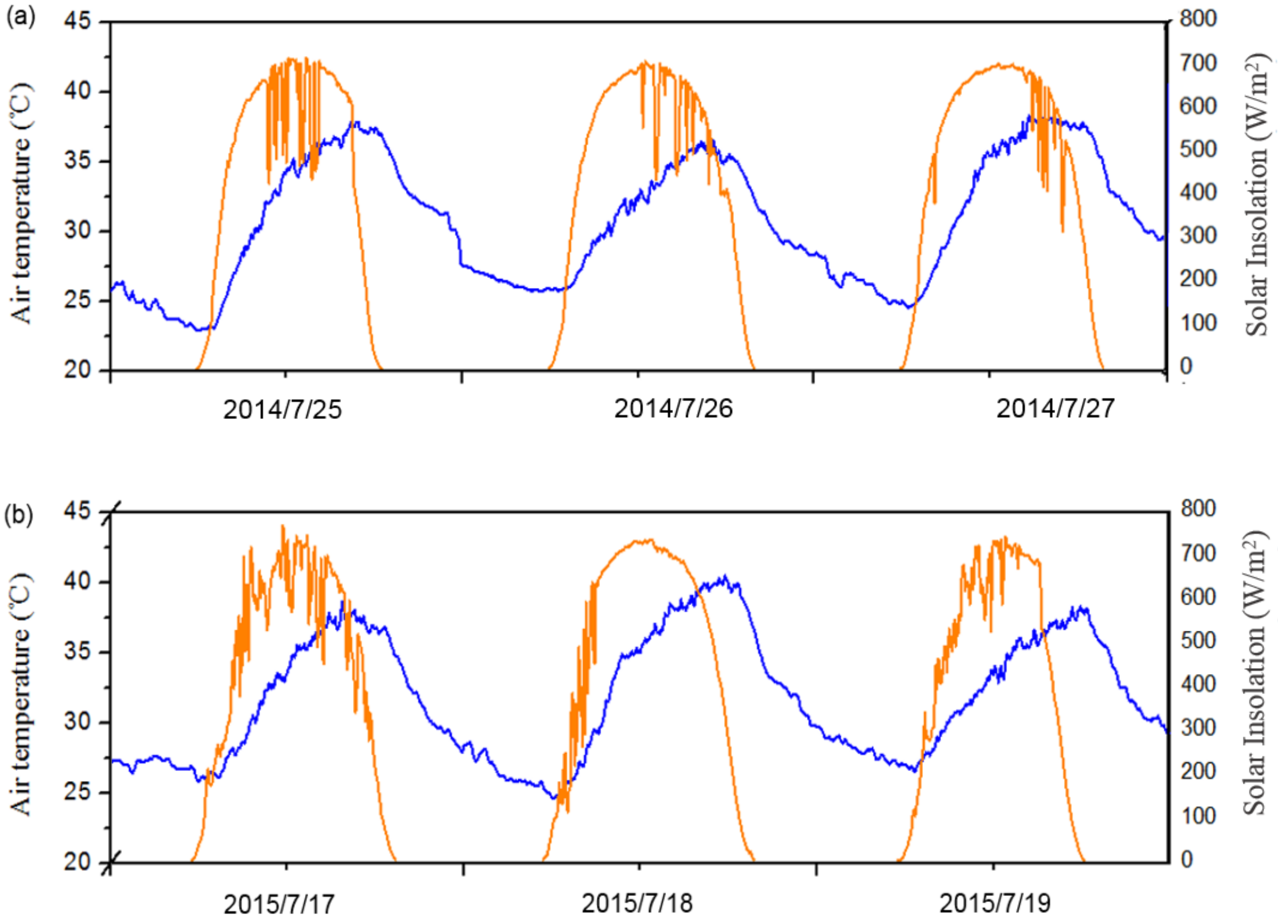

Figure 10 Outdoor solar irradiation and air temperature.

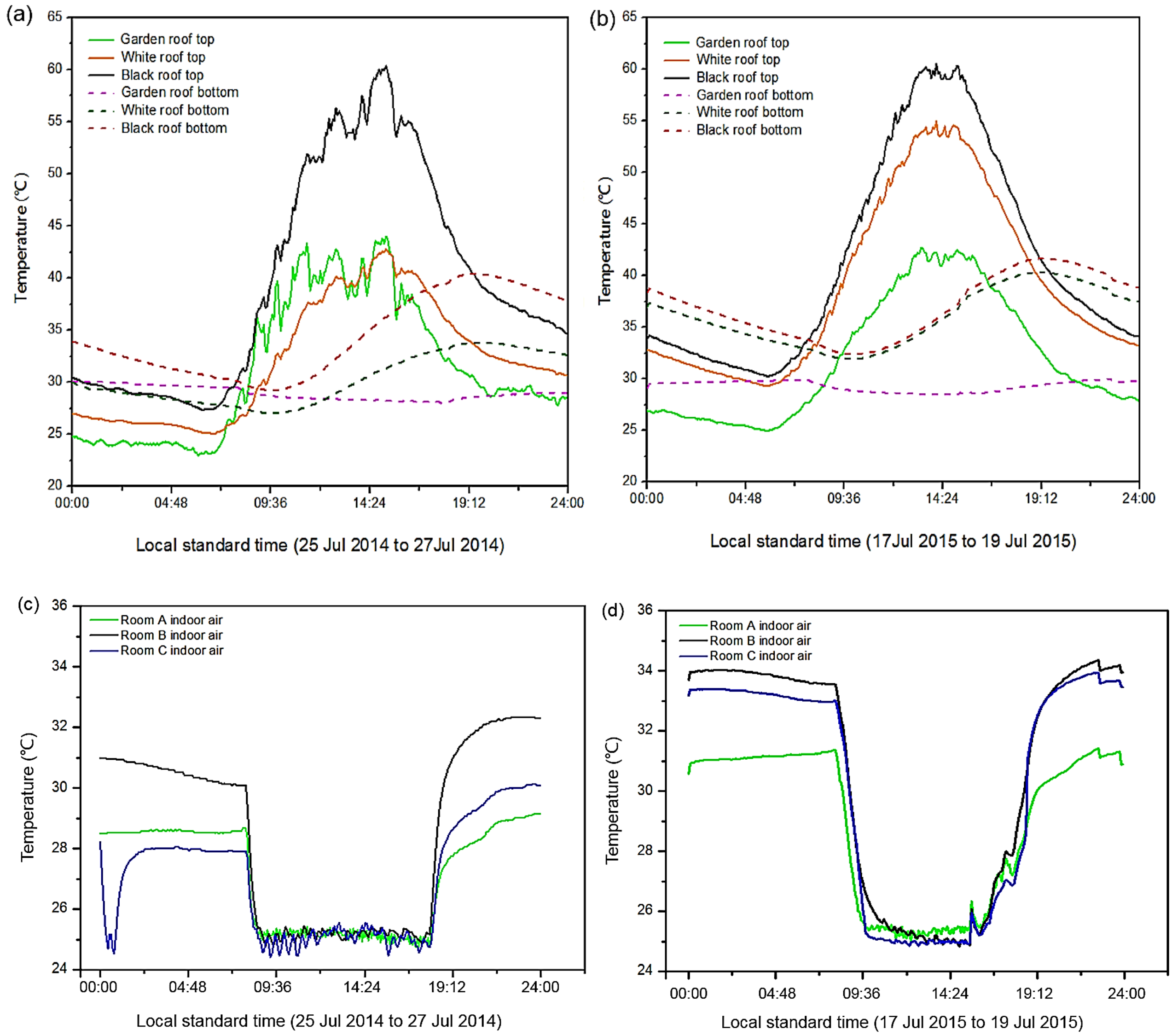

Figure 11 Temperature distributions of roofs (a, b); and indoor air temperature (c, d).

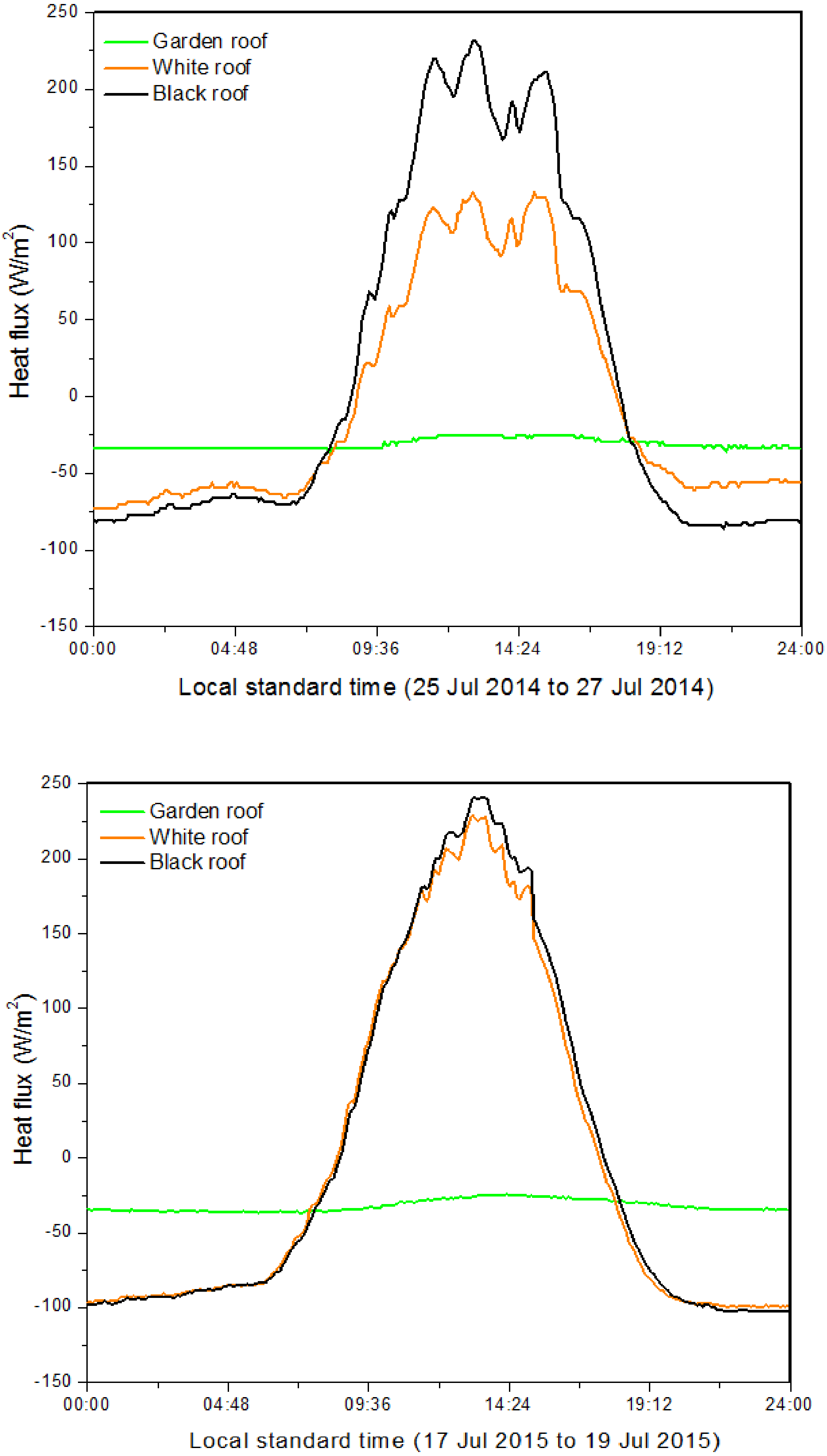

Figure 12 Heat fluxes through the exterior surfaces of the roofs.

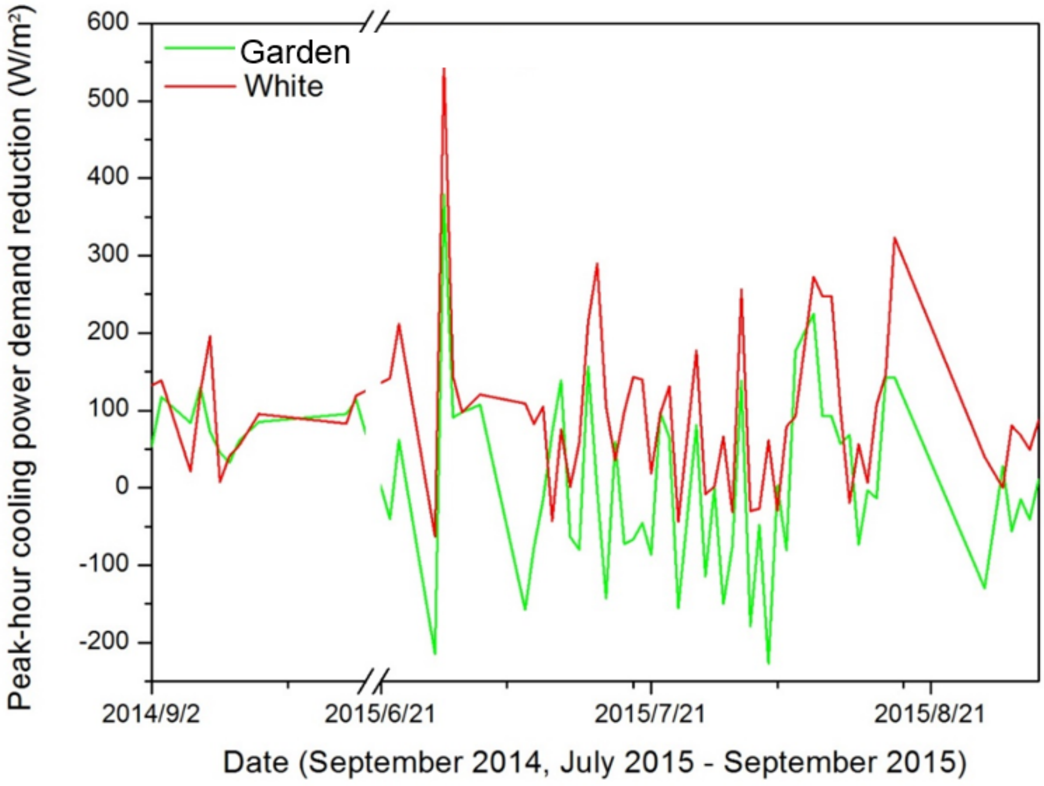

Figure 13 Daily values of peak-hour cooling power demand reduction.

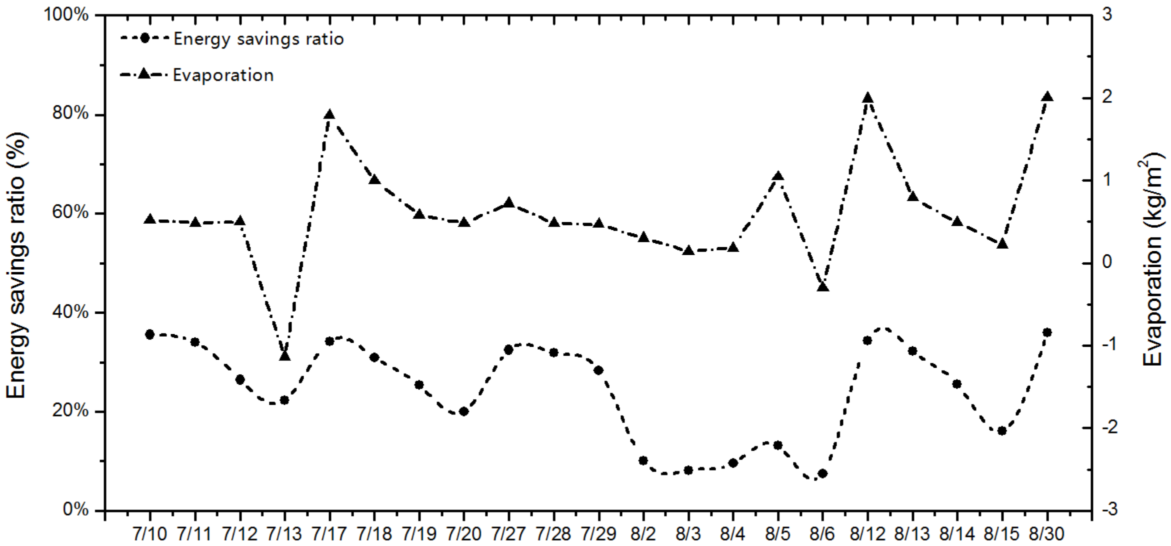

Figure 14 Energy savings ratio and evaporation of the sedum-tray garden roof [3].

[3] Energy savings ratio is the energy savings of room A/power consumption of room B

Table captions

Table 1 Description of sedum lineare planting modules.

Table 2 Characteristics of the test rooms in the office building in the Jiangjin District of Chongqing.

Table 3 Measurement sensors and protocol in an office building in Jiangjin District, Chongqing.

Table 4 Roof top and bottom temperatures and peak heat fluxes of rooms on the summer and winter days.

Table 5 Seasonal and annual mean values of energy savings and emission reduction.

Table 6 Roof top and bottom temperature reductions in 2014 and 2015.

Table 1 Description of Sedum lineare planting modules.

Item	Index
Planting modules	Sedum + nutritional soil + filter + storage / hydrophobic sand + EPS boards
Geometric Size (mm)	500 x 500 x 90
Planting load (kg/m^2)	35
Thermal resistance ($m^2 \cdot K/W$)	0.857
Regenerative coefficient[4] ($W/m^2 \cdot K$)	1.6
Sedum growth height (mm)	80–100
Sedum growth diameter (mm)	60–80
Planting density (plants per module)	20–25
Leaf area index	2.9
Life expectancy (y)	10–20

[4] Regenerative coefficient is the ability of the materials to store heat.

Table 2 Characteristics of the test rooms in the office building in the Jiangjin District of Chongqing.

Roof type	Room A	Room B	Room C
	Sedum-tray garden roof	Black roof	White roof
Initial solar reflectance	0.36	0.21	0.84
Installation date	2014-08-15	same	same
Products and manufacturers	Guangdong Shunguan Waterproof Reinforcement Engineering Co., LTD. SGK Sedum lineare planting module	Chongqing Gongmei Science and Technology Development Co., LTD. AL-6001 Black Roofing System	Chongqing Aluo Science and Technology Development Co., LTD. AL-8001 Cool Roofing System
Coating material	Sedum + 1.5-4.0 cm depth of nutritional soil + filter + 2 cm storage / hydrophobic sand + EPS board	Polyurethane waterproof coating	Ceramic glaze with titanium silicon cenosphere filler
Roof structure (layers, top to bottom)	5 mm waterproofing membrane + 20 mm cement mortar + 45 mm EPS+ 20-mm cement mortar + 20 mm slag cement + 120 mm reinforced concrete+20 mm cement mortar	Same	Same
Roof assembly thermal resistance (m^2 K/W)	1.02	Same	Same
Floor & roof area (m^2)	21.4	Same	Same
Ceiling height (m)	3.3	Same	Same
Doors (number, total area [m^2])	1, 1.89	Same	Same
Windows (number, orientation, window-wall ratio, total area [m^2])	2, south, 0.17, 2	Same	Same
Cooling/heating equipment	Split-system direct expansion air-source heat pump	Same	Same
Make and model	Media KFR-35GW/DY-IA(R3)	Same	Same
COP	3.29(Summer)/3.67(Winter)	Same	Same
Capacity (W)	3,520(Summer)/4,000(Winter)	Same	Same
Set point (°C)	26(Summer)/20(Winter)	Same	Same
Schedule	08:00–18:00 (Workdays)	Same	Same

Table 3 Measurement sensors and protocol in an office building in Jiangjin District, Chongqing.

Measurement	Details
Roof top, bottom, soil, ceiling, and interior wall temperature	
Sensor type	Temperature (resistance temperature detector)
Sensor make	Pt100
Sensor range/accuracy	−40–150 °C / 0.2 °C
Protocol	Sensor totally encased in the roof top and painted the same color as the corresponding roof coating; sensor attached to the surface of the roof bottom, soil, ceiling, and interior wall and affixed using aluminum foil
Roof top heat flux	
Sensor type	Heat flux sensor
Sensor model	HFP01-10
Sensor range/accuracy	−2,000–2,000 W/m^2/ < 5 %
Protocol	Sensor totally encased in the roof top, layered with thermally conductive paste and cement plaster, and painted the same color as the corresponding roof coating
Soil moisture	
Sensor type	Soil moisture sensor
Sensor model	TDR-3
Sensor range/accuracy	0–100 %(m^3/ m^3) / ± 2 %
Protocol	Sensor totally embedded in the soil
Single module weight	
Sensor type	Soil moisture sensor
Sensor model	TDR-3
Sensor range/accuracy	0–100 %(m^3/ m^3) / ± 2 %
Protocol	Sensor placed in the middle of the module
Outside air, indoor air temperature	
Sensor type	Weighting sensor
Sensor model	CZ-1
Sensor range/accuracy	0–15 kg / 0.5 g
Protocol	Sensor suspended 1.5 m above floor; measurement logged internally every 5 minutes
Global horizontal, diffuse solar irradiance	
Sensor type	Solar radiation recorder
Sensor model	PC-2
Sensor range / accuracy	280–3000nm / 0.5 %
Protocol	Sensor suspended 1.5 m above floor and installed horizontally on roof top
Cooling + heating electricity use	
Sensor type	Power meter
Sensor model	PowerBay-T8005
Sensor range/accuracy	0–2.2 kW/0.1 kW
Reflectance of roofs	
Sensor type	Reflectance sensor
Sensor model	TDR-3
Spectral range	300–3000 nm
Sensor range/ accuracy	0–100 % (m^3 / m^3) / ± 2 % (m^3 / m^3)
Protocol	Sensor is covered with 2 layers of quartz glass and suspended 1.5 m above and installed horizontally on roof top

Table 4 Roof top and bottom temperatures and peak heat fluxes of rooms on the summer and winter days.

Roof type		Room A	Room B	Room C
		Sedum-tray garden roof	Black roof	White roof
Summer day	Maximum roof top temperature (°C)	47.1	58.2	42.2
	Maximum bottom temperature (°C)	27.7	39.0	32.1
	Peak heat flux (W/m^2)	−27.0	236.0	183.0
Winter day	Maximum roof top temperature (°C)	28.7	33.9	30.9
	Maximum bottom temperature (°C)	24.7	26.7	24.5
	Peak heat flux (W/m^2)	−32.0	109.0	98.0

Table 5 Seasonal and annual mean values of energy savings and emission reduction.

Savings per unit conditioned roof area	Cooling season (2014.09; 2015.06 to 2015.09)		Heating season (2014.11 to 2015.02)		Annual	
	White roof	Sedum-tray garden roof	White roof	Sedum-tray garden roof	White roof	Sedum-tray garden roof
Daily cooling energy (Wh/m^2)	74.5	89.0	—	—	—	—
Daily heating energy (Wh/m^2)	—	—	−11.3	−40.2	—	—
Seasonal or annual energy (kWh/m^2)	4.8	5.7	−0.9	−3.2	3.9	2.5
Seasonal or annual conditioning energy cost (RMB/m^2)	4.1	4.8	−0.8	−2.7	3.3	2.1
Seasonal or annual CO_2 (kg/m^2)	4.0	4.7	−0.7	−2.6	3.2	2.1
Seasonal or annual NO_x (g/m^2)	22.0	26.1	−4.1	−14.7	17.9	11.4
Seasonal or annual SO_2 (g/m^2)	53.3	63.3	−10.0	−35.5	43.3	27.8

Table 6 Roof top and bottom temperature reductions in 2014 and 2015.

Temperature		Roof top (°C)		Roof bottom (°C)	
		Black−white	Black−garden	Black−white	Black−garden
2014	Max	17.6	16.4	6.6	10.3
	Mean	7.6	8.5	4.2	5.5
2015	Max	5.6	17.9	1.3	11.7
	Mean	2.4	9.5	0.9	7.7